The Scientific World Journal

Knee Joint Biomechanics in High Flexion

Guest Editors: Shunji Hirokawa, Kazuo Kiguchi, Mitsugu Todo, Bharat Mody, and Ashvin Thambyah

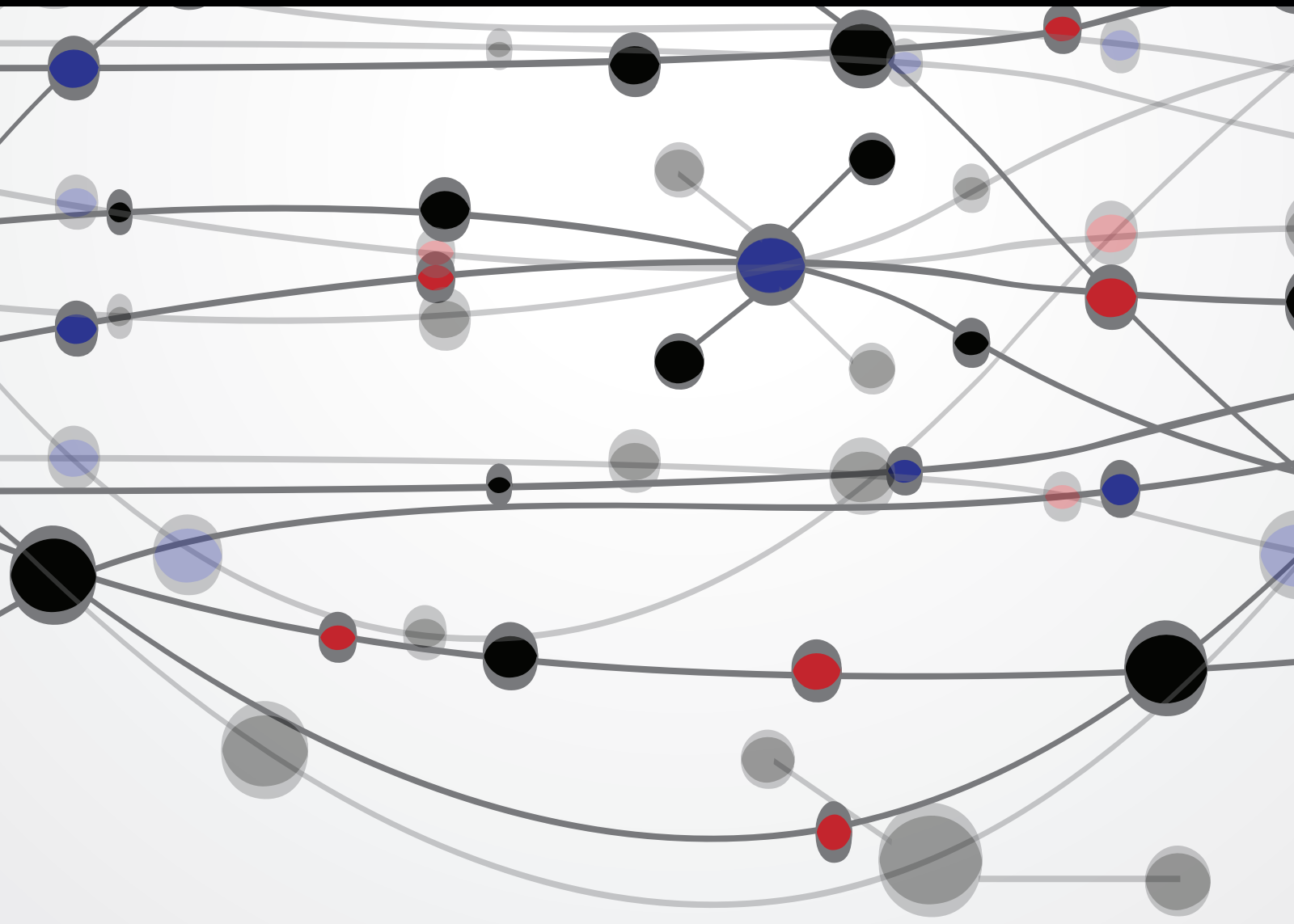

Knee Joint Biomechanics in High Flexion

The Scientific World Journal

Knee Joint Biomechanics in High Flexion

Guest Editors: Shunji Hirokawa, Kazuo Kiguchi, Mitsugu Todo, Bharat Mody, and Ashvin Thambyah

Contents

Hindawi Publishing Corporation
The Scientific World Journal
Volume 2014, Article ID 459408, 2 pages
http://dx.doi.org/10.1155/2014/459408

Editorial

Knee Joint Biomechanics in High Flexion

Shunji Hirokawa,[1] Kazuo Kiguchi,[2] Mitsugu Todo,[3] Bharat Mody,[4] and Ashvin Thambyah[5]

[1] *Research Center for Advanced Biomechanics, Kyushu University, 744 Motooka, Nishi-ku, Fukuoka 819-0395, Japan*
[2] *Department of Mechanical Engineering, Faculty of Engineering, Kyushu University, 744 Motooka, Nishi-ku, Fukuoka 819-0395, Japan*
[3] *Division of Renewable Energy Dynamics, Research Institute for Applied Mechanics, Kyushu University, Kasuga-koen, Kasuga, Fukuoka 816-8580, Japan*
[4] *Welcare Hospital, Akashganga Complex, Race Course Circle, Baroda, Gujarat 390 007, India*
[5] *Department of Chemical and Materials Engineering, Faculty of Engineering, University of Auckland, Symonds Street, Auckland 1010, New Zealand*

Correspondence should be addressed to Shunji Hirokawa; hirokawa@mech.kyushu-u.ac.jp

Received 12 June 2014; Accepted 12 June 2014; Published 17 July 2014

A complete understanding of joint biomechanics is important in the diagnosis of joint disorders, in the quantitative assessment of treatment outcomes, and in the improvement of prosthetic devices. Yet, there is little data on high flexion activities, despite the fact that these activities are considered not only crucial to people in Asia and the Middle East, but also necessary to people in the West for improving their quality of life. Thus, we planned to invite investigators to contribute original research articles as well as review articles that will stimulate the continuing efforts to develop a thorough knowledge base for biomechanics of the knee joint during demanding activities of daily living.

To this end, the special issue has been posted online on the journal's website, in which the following articles are offered for public viewing.

"*Squatting-related tibiofemoral shear reaction forces and a biomechanical rationale for femoral component loosening*" by A. Thambyah and J. Fernandez deduces that the rapid reversal of the tibiofemoral shear force from the posterior to the anterior direction from knee extension to high flexion, respectively, may cause the femoral component loosening of high flexion implants. In this article, the results from biomechanical and finite element analyses clearly explain the relationship between the femoral loosening and frequent squatting.

"*The effect of malrotation of tibial component of total knee arthroplasty on tibial insert during high flexion using a finite element analysis*" by K. Osano et al. pertains to the finite element analysis to study the effect of malrotation of tibial component on tibial insert during squatting maneuver. Three different tibial rotations (15° internal, normal, 15° external) were set as the initial conditions for analyses. Then it was found that when the tibia was internally rotated the insert had such high stress as 160% of normal position. It was concluded that internal malrotation should be avoided as much as possible.

"*Biomechanical considerations in the design of high-flexion total knee replacements*" by C.-K. Cheng et al. is the review article in which the authors share several experiences in the previous literature for biomechanical and kinematic performance of knee prostheses under the specific demand for high flexion of knee joint. For achieving deep knee flexion, some ideas are discussed such as a rounded and convex lateral plateau and a shallower medial plateau on the tibial surface, a rounded postcam contact surface, and an asymmetric curve-on-curve cam shape.

"*Dynamic finite element analysis of mobile bearing type knee prosthesis under deep flexional motion*" by M. A. M. Anuar et al. also pertains to the finite element analysis to distinguish the mechanical performances between mobile

bearing and fixed bearing posterior stabilized knee prostheses. Then this study shows the decomposition of multidirectional motion to unidirectional kinematics of femoral-insert and insert-tray articulating interfaces in mobile bearing TKA in maintaining lower stress at tibial condylar.

"*Modelling and analysis on biomechanical dynamic characteristics of knee flexion movement under squatting*" by J. Wang et al. represents the results from the synchronal measurements of both kinematics and contact stresses, respectively, for the tibiofemoral and patellofemoral joints. Dynamic finite element analysis and in vitro experiment were carried out for the range from full extension to squatting of the knee. Comparative study between their results and the literature data is comprehensive.

We hope that the above articles are of interest to the reader and more articles would be incorporated in this special issue.

Shunji Hirokawa
Kazuo Kiguchi
Mitsugu Todo
Bharat Mody
Ashvin Thambyah

Hindawi Publishing Corporation
The Scientific World Journal
Volume 2014, Article ID 586921, 6 pages
http://dx.doi.org/10.1155/2014/586921

Research Article

Dynamic Finite Element Analysis of Mobile Bearing Type Knee Prosthesis under Deep Flexional Motion

Mohd Afzan Mohd Anuar,[1,2] Mitsugu Todo,[3] Ryuji Nagamine,[4] and Shunji Hirokawa[5]

[1] *Interdisciplinary Graduate School of Engineering Sciences, Kyushu University, 6-1 Kasuga-koen, Kasuga 816-8580, Japan*
[2] *Faculty of Mechanical Engineering, Universiti Teknologi MARA, 40450 Shah Alam, Selangor, Malaysia*
[3] *Research Institute for Applied Mechanics, Kyushu University, 6-1 Kasuga-koen, Kasuga 816-8580, Japan*
[4] *Sugioka Memorial Hospital, 3-6-1 Kashiiteriha, Higashi Ward, Fukuoka, Fukuoka Prefecture 813-0017, Japan*
[5] *Biomechanics Research Center, Kyushu University, 744 Motooka, Nishi-ku, Fukuoka 819-0395, Japan*

Correspondence should be addressed to Mitsugu Todo; todo@riam.kyushu-u.ac.jp

Received 14 March 2014; Accepted 22 May 2014; Published 17 July 2014

Academic Editor: Ashvin Thambyah

The primary objective of this study is to distinguish between mobile bearing and fixed bearing posterior stabilized knee prostheses in the mechanics performance using the finite element simulation. Quantifying the relative mechanics attributes and survivorship between the mobile bearing and the fixed bearing prosthesis remains in investigation among researchers. In the present study, 3-dimensional computational model of a clinically used mobile bearing PS type knee prosthesis was utilized to develop a finite element and dynamic simulation model. Combination of displacement and force driven knee motion was adapted to simulate a flexion motion from 0° to 135° with neutral, 10°, and 20° internal tibial rotation to represent deep knee bending. Introduction of the secondary moving articulation in the mobile bearing knee prosthesis has been found to maintain relatively low shear stress during deep knee motion with tibial rotation.

1. Introduction

Introduction of mobile insert is believed to decrease polyethylene (PE) wear and facilitate range of motion (ROM) as well as tibial axial rotation by appearance of second moving interfaces between tibial insert and tibial tray [1, 2]. The advantage of this feature, however, is still in doubt and remains in further investigation. To the best of our knowledge, there is no apparent evidence of superiority of one design over another revealed in previous short-term and midterm clinical studies [2–5]. In these studies, mobile and fixed bearing knee prostheses were analyzed based on various attributes including Knee Score, Function Score, maximum flexion, pain score, and ROM. This observation is supported by *in vitro* assessments through wear analysis which is unable to disclose any significant difference in wear rate between mobile and fixed bearing PE insert [6]. Though, this result is contradicting with work by McEwen et al. who adapted comparable method and found obviously lower wear rate in mobile insert in comparison to fixed bearing tibial insert [7]. Good agreement with this study, however, was addressed by Sharma et al. who compared *in vivo* contact stress in the mobile bearing with the fixed bearing prostheses. They concluded that mobile bearing design capable of maintaining high conformity results in lower contact stress in comparison to fixed bearing design [8].

This study attempts to compare kinetics behavior of tibial condylar between mobile bearing and fixed bearing PE insert under dynamic loaded deep knee bending and tibial rotation.

2. Method and Analysis

A 3D computational geometry of Japanese company commercially developed PS type mobile bearing knee prosthesis

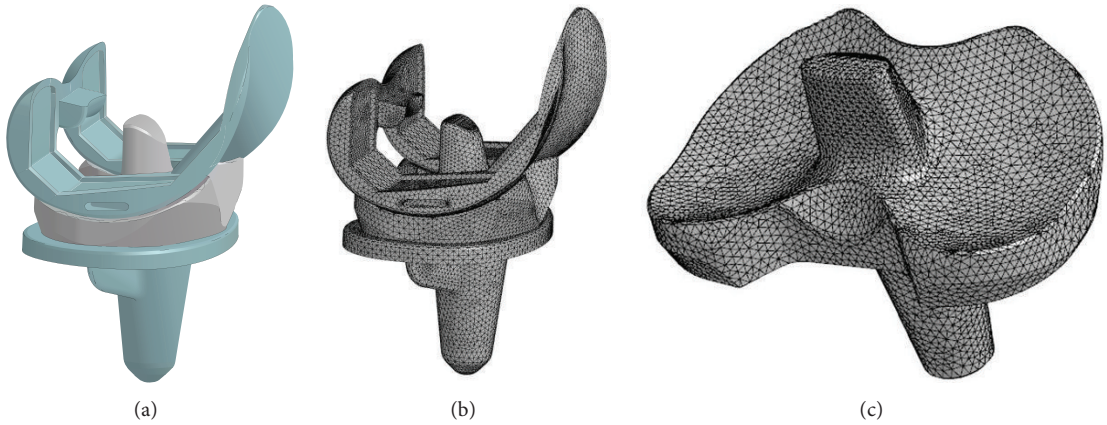

(a) (b) (c)

Figure 1: Computational models of mobile bearing type knee prosthesis. (a) CAD model, (b) Mesh model, and (c) Mesh model of tibial insert.

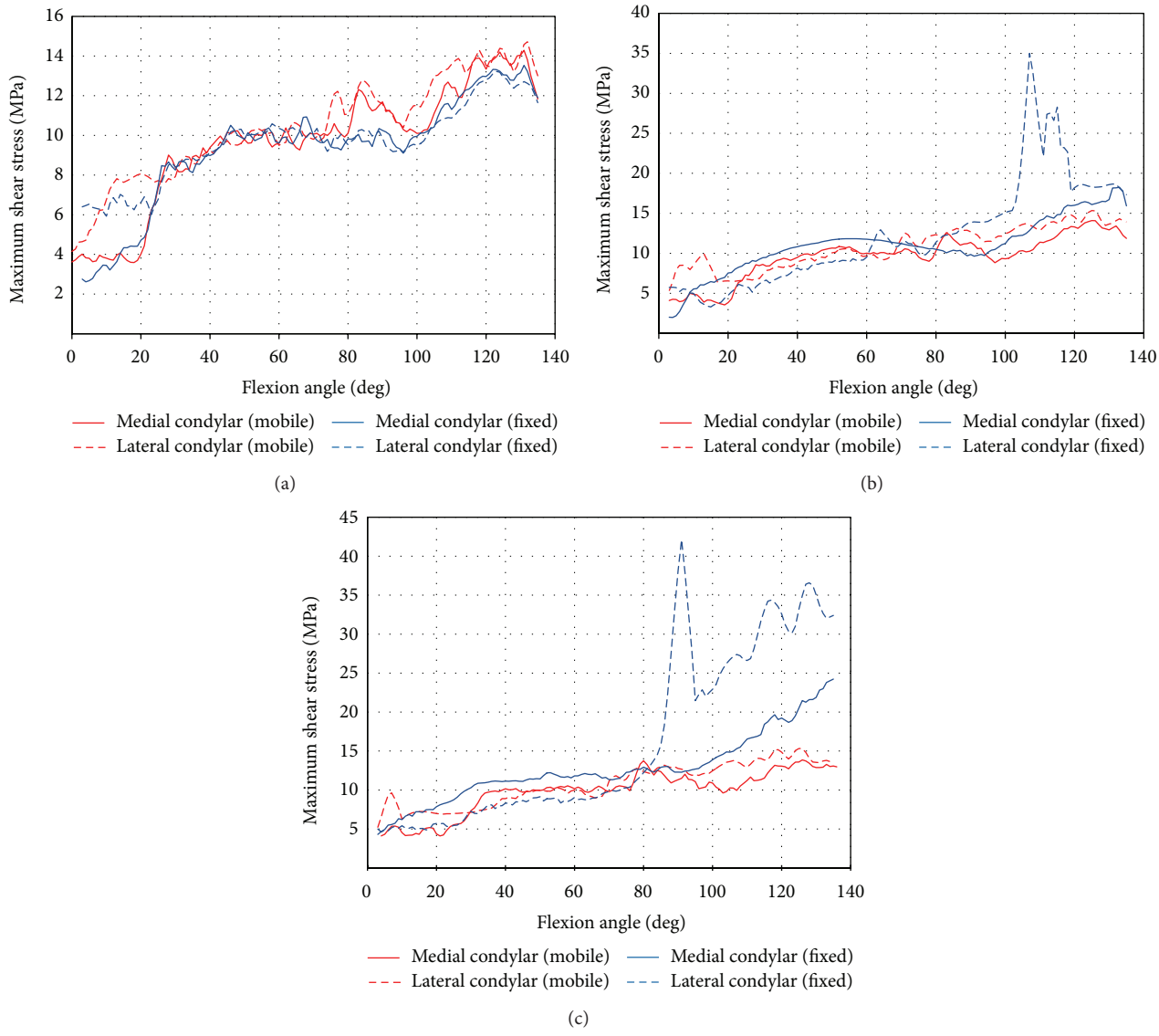

Figure 2: Maximum shear stress history from 0° to 135° of flexion angle. (a) Neutral position. (b) 10° tibial rotation. (c) 20° tibial rotation.

Table 1: Peak contact stress, mean contact stress, and contact area with neutral position at 90° and 120° of flexion angles.

Flexion angle (°)	Peak contact stress (MPa)		Mean contact stress (MPa)		Contact area (mm^2)	
	FE model	Nakayama et al. [9]	FE model	Nakayama et al. [9]	FE model	Nakayama et al. [9]
90	27.3	25.9 ± 1.5	13.0	11.1 ± 0.2	42.6	45.1 ± 2.1
120	27.7	32.4 ± 0.5	12.4	14.8 ± 0.5	38.6	45.1 ± 2.1

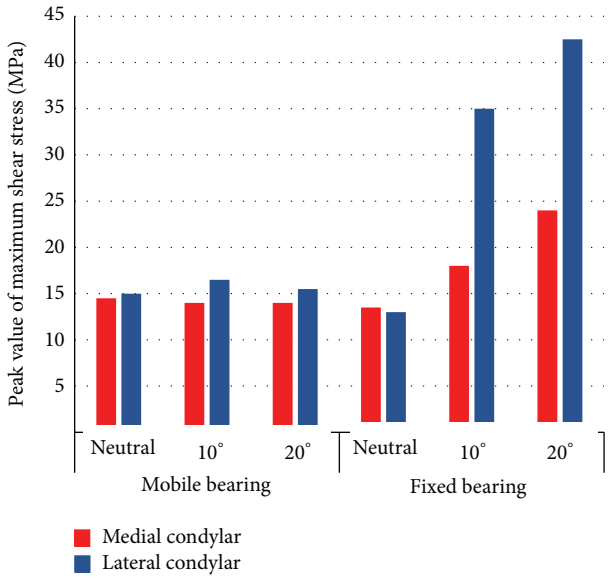

Figure 3: Peak values of maximum shear stress for mobile and fixed bearing TKA at neutral, 10°, and 20° internal tibial rotation.

was used to construct a finite element (FE) model in FEMAP using 1.2 mm of edge length tetrahedron element (123,468 elements) with 32,436 nodes as shown in Figure 1. Femoral component and tibial tray were modelled as rigid bodies due to significantly higher Young's Modulus than mobile insert which was represented by an elastic-plastic material (E = 800 MPa) with Poisson's ratio of 0.40. The static and dynamic coefficients of friction of metal-on-plastic contact were selected as 0.04 [10, 11]. Penalty-based algorithm was used for contact definition. The FE model has been validated using NRG knee prosthesis model which applied similar model setup. The peak contact stress, mean contact stress, and contact area at 90° and 120° of flexion with neutral rotation of FE model were compared with results from previous work by Nakayama et al. [9].

The dynamic model was developed in LS-Dyna. Soft tissues constraint around the knee was represented by a pair of nonlinear springs inserted both anteriorly and posteriorly. The spring force in function of displacement can be expressed by

$$F = k_1 d^2 + k_2 d = 0.18667\, d^2 + 1.3313\, d, \quad (1)$$

where F is the force exerted, d is the spring displacement, and k_1 and k_2 are the stiffness coefficients of the springs, respectively [12]. The combination of displacement and force driven knee joint was adapted to perform dynamic motion of the 6-degree-of-freedom prosthesis model. The femoral component was constrained in mediolateral (ML) displacement, anteroposterior (AP) displacement, and rotation, as well as proximodistal (PD) rotation, while being driven by flexional motion about ML-axis from 0° to 135° of angle. The vertical load from previous experimental work by Dahlkvist et al. was applied to the femoral component [13]. The tibial tray was constrained in PD displacement and ML rotation, while AP displacement was driven by AP force obtained from the same literature. At the same instance, the tray was set to perform axial rotation about PD-axis with neutral, 10°, and 20° of maximum tibial angle, respectively, to represent tibial rotation. Similar prosthesis model was used to represent fixed bearing design by fixing the mobile insert to the tibial tray to eliminate the effect of implant geometry.

3. Results

The comparison of results between FE model and experimental work by Nakayama et al. is shown in Table 1. The greatest differences of peak contact stress, mean contact stress, and contact area were 14.5%, 17.1%, and 7.9%, respectively, demonstrating a good agreement between both results. The maximum shear stress at medial and lateral tibia condyles in the function of flexion angle for neutral, 10°, and 20° tibial rotation, respectively, is illustrated in Figure 2. It was noted that the maximum shear stress at both medial and lateral condyles for neutral rotation increased with flexion angle. Similar trend was exhibited for the tibia which underwent 10° and 20° axial rotations. However, shear stress of mobile bearing insert was found less sensitive to tibial rotation in comparison to fixed bearing design where the maximum shear stress at both condyles varied from 5 MPa to 15 MPa for all conditions of tibial rotations.

Figure 3 shows the comparison of peak values of maximum shear stress between medial and lateral condyles with respect to tibial rotation and type of bearing mobility. Overall, peak values of maximum shear stress at lateral condylar were found relatively higher than medial condylar. As for fixed bearing insert which underwent axial rotation, the peak values at lateral condylar increased greater as compared with medial condylar. The peak values at medial condylar rose from 13.5 MPa with neutral position to 18 MPa and 24 MPa with 10° and 20° of tibial rotations, respectively. Meanwhile, at lateral condylar, increments from 13 MPa with neutral position to 35 MPa and 42.5 MPa with 10° and 20° of tibial rotations, respectively, were observed. On the contrary, for mobile bearing insert, the peak values remained around 14 MPa to 16 MPa at both condyles even subjected to axial rotational motion.

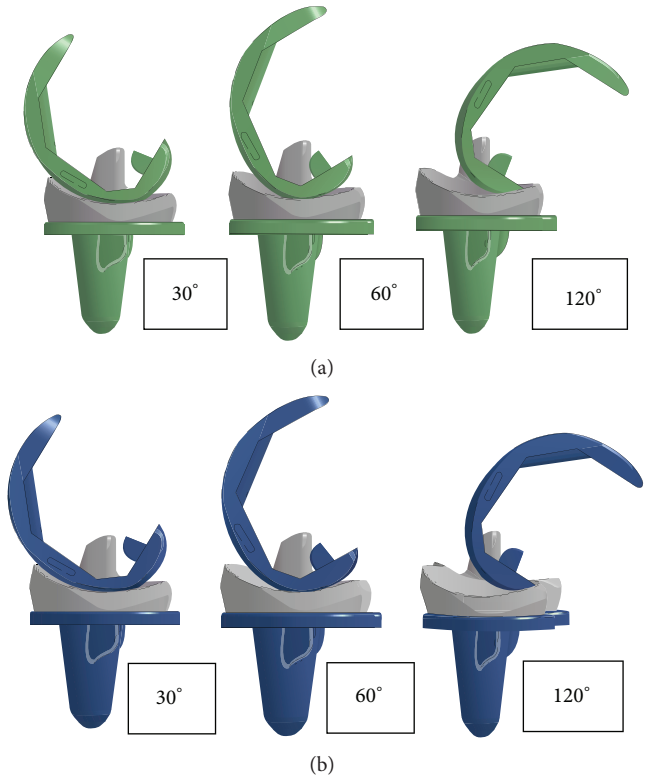

Figure 4: Lateral view of TKA during 30°, 60°, and 120° of flexion angle. (a) Mobile bearing. (b) Fixed bearing.

4. Discussion

4.1. Mechanics of Knee during Deep Flexional Motion. Most TKA postoperative patients especially in Asian countries may anticipate ability of deep kneeling which is associated with cultural and religious activities such as *seiza* among Japanese and kneeling in prayer for Muslims. Numerous studies have reported the critically large loadings generated at knee joint during deep bending motion. Dahlkvist et al. analyzed knee joint forces on six subjects and concluded that up to more than 5 times bodyweight of normal force is induced at tibiofemoral articulations during rapid descending [13]. In other investigations, single leg squatting was estimated to generate about 8% bodyweight of net normal force at knee joint [14]. Knee kinematics of high flexion analysis in previous works have showed the increasing tibial rotation up to 11° at 150° of flexion angle in intact knee and maximum of 17° at 137° of flexion angle in TKA postoperative knee [15, 16]. Excessive load combined with this state of motion may generate considerably high stress which, in turn, results in wear and delamination at articular surface of tibial insert as this study has shown relatively high shear stress, ranging from 10 to 50 MPa, induced at insert condylar during deep squatting.

4.2. Shear Stress States at Tibial Condylar. Wear and delamination of PE insert are among the most common problems in TKA that limit the survivorship of the prostheses. This defect is generated by excessive shear stress, contact pressure, and cross-shear associated with tibiofemoral contact geometry [15, 16]. Lower contact area in less conforming TKA results in higher contact pressure and shear stress relative to high conformity TKA. During femoral rollback, tibiofemoral contact shifts from larger contact area at centre of condylar to smaller contact area at posterior sides of both medial and lateral condyles leading to increasing shear stress with increasing flexion angle. Comparable mechanism happens in both mobile and fixed bearing TKAs as shown in Figure 4. As the knee flexes, medial femoral condylar moves anteriorly and lateral femoral condylar moves posteriorly causing internal rotation of tibia. Larger anterior surface relative to posterior on both tibia condyles leads to higher shear stress created at lateral condylar during deep bending motion. For fixed bearing condition, tremendous increment of shear stress at higher flexion angle (90°–110°) occurred due to impingement between femoral component and posterior articular surface of lateral condylar.

4.3. Mobile Bearing versus Fixed Bearing: Stress Sensitivity towards Knee Motion. Mobile bearing TKA is found less sensitive towards tibial rotation in terms of shear stress as compared with fixed bearing TKA. During tibia rotation, tibia transmits axial loading to tibial tray. In mobile bearing TKA design, kinematics of knee is uncoupled into two unidirectional motions by introducing second insert-tray articulations. Due to tibiofemoral engagement at proximal

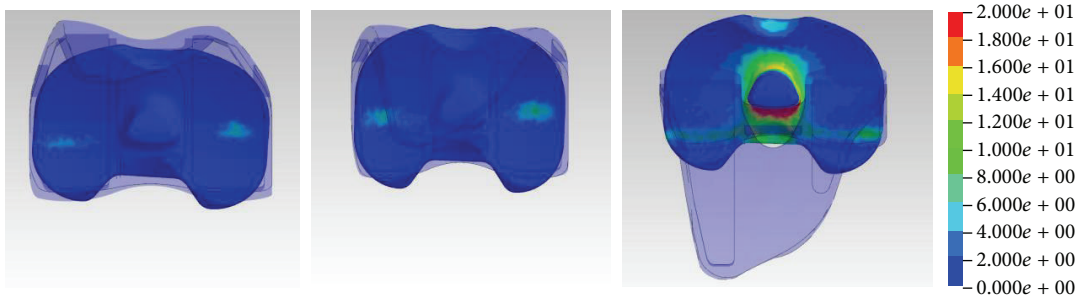

(a) Plane view of mobile insert

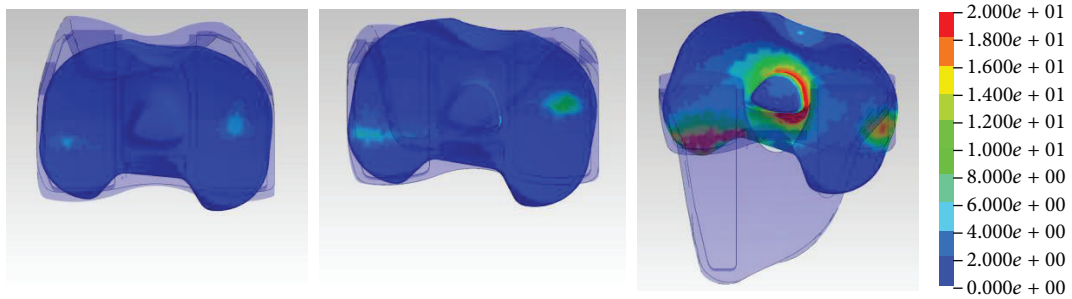

(b) Plane view of fixed insert

FIGURE 5: Shear stress distribution on the plane views of mobile and fixed inserts at 30°, 60°, and 120° of flexion angle, respectively, depicting the shear stress distribution. The fringe level is displayed in the unit of MPa.

articular surface, the mobile insert maintains its neutral position and results in relatively lower shear stress at tibial condylar (Figure 5). In fixed bearing TKA, axial loading from tibial tray is transmitted evenly to tibial insert causing high shear stress generated on both medial and lateral condyles. Furthermore, multidirectional motion experienced by proximal surface of fixed insert will induce more wear and delamination. This result is supported by *in vitro* wear study by McEwen et al. who suggested that distribution of motions into femoral-insert and insert-tray interfaces in mobile bearing TKA has produced lower mobile insert wear defect [7]. Figure 5(b) illustrates the shear stress distribution in fixed insert at 30°, 60°, and 120°, respectively. It can be noted that the shear stress shifts from centre of condylar to posterior side of lateral condylar. However, research by Engh et al. revealed that appearance of second articulating surfaces introduced supplementary source of wear [17]. Existence of wear debris may alter the surface friction which is attributed to frictional force transmission from tibial tray to PE insert, hence affecting the stress states at upper side of tibial insert. This circumstance was not considered in the present study.

5. Conclusions

In conclusion, this study has showed the decomposition of multidirectional motion to unidirectional kinematics of femoral-insert and insert-tray articulating interfaces in mobile bearing TKA capable of maintaining lower stress at tibial condylar. Further investigation should be performed on various designs of mobile bearing TKAs to observe reproduction of this insert-tray mobility effect on stress states of tibial condylar.

Conflict of Interests

The authors declare that there is no conflict of interests regarding the publication of this paper.

Acknowledgment

This work was partially supported by JSPS KAKENHI Grant no. 24300201.

References

[1] Z. D. Post, W. Y. Matar, T. van de Leur, E. L. Grossman, and M. S. Austin, "Mobile-bearing total knee arthroplasty. Better than a fixed-bearing?" *Journal of Arthroplasty*, vol. 25, no. 6, pp. 998–1003, 2010.

[2] W. C. H. Jacobs, B. Christen, A. B. Wymenga et al., "Functional performance of mobile versus fixed bearing total knee prostheses: a randomised controlled trial," *Knee Surgery, Sports Traumatology, Arthroscopy*, vol. 20, no. 8, pp. 1450–1455, 2012.

[3] G. R. Scuderi, D. R. Hedden, J. A. Maltry, S. M. Traina, M. B. Sheinkop, and M. A. Hartzband, "Early clinical results of a high-flexion, posterior-stabilized, mobile-bearing total knee arthroplasty: a US investigational device exemption trial," *The Journal of Arthroplasty*, vol. 27, no. 3, pp. 421–429, 2012.

[4] S. Bhan, R. Malhotra, E. K. Kiran, S. Shukla, and M. Bijjawara, "A comparison of fixed-bearing and mobile-bearing total knee

arthroplasty at a minimum follow-up of 4.5 years," *Journal of Bone and Joint Surgery A*, vol. 87, no. 10, pp. 2290–2296, 2005.

[5] P. Aglietti, A. Baldini, R. Buzzi, D. Lup, and L. de Luca, "Comparison of mobile-bearing and fixed-bearing total knee arthroplasty: a prospective randomized study," *Journal of Arthroplasty*, vol. 20, no. 2, pp. 145–153, 2005.

[6] H. Haider and K. Garvin, "Rotating platform versus fixed-bearing total knees: an in vitro study of wear," *Clinical Orthopaedics and Related Research*, vol. 466, no. 11, pp. 2677–2685, 2008.

[7] H. M. J. McEwen, P. I. Barnett, C. J. Bell et al., "The influence of design, materials and kinematics on the in vitro wear of total knee replacements," *Journal of Biomechanics*, vol. 38, no. 2, pp. 357–365, 2005.

[8] A. Sharma, R. D. Komistek, C. S. Ranawat, D. A. Dennis, and M. R. Mahfouz, "In vivo contact pressures in total knee arthroplasty," *Journal of Arthroplasty*, vol. 22, no. 3, pp. 404–416, 2007.

[9] K. Nakayama, S. Matsuda, H. Miura, H. Higaki, K. Otsuka, and Y. Iwamoto, "Contact stress at the post-cam mechanism in posterior-stabilised total knee arthroplasty," *Journal of Bone and Joint Surgery B*, vol. 87, no. 4, pp. 483–488, 2005.

[10] A. C. Godest, M. Beaugonin, E. Haug, M. Taylor, and P. J. Gregson, "Simulation of a knee joint replacement during a gait cycle using explicit finite element analysis," *Journal of Biomechanics*, vol. 35, no. 2, pp. 267–275, 2002.

[11] J. P. Halloran, A. J. Petrella, and P. J. Rullkoetter, "Explicit finite element modeling of total knee replacement mechanics," *Journal of Biomechanics*, vol. 38, no. 2, pp. 323–331, 2005.

[12] S. Sathasivam and P. S. Walker, "Computer model to predict subsurface damage in tibial inserts of total knees," *Journal of Orthopaedic Research*, vol. 16, no. 5, pp. 564–571, 1998.

[13] N. J. Dahlkvist, P. Mayo, and B. B. Seedhom, "Forces during squatting and rising from a deep squat," *Engineering in Medicine*, vol. 11, no. 2, pp. 69–76, 1982.

[14] T. Nagura, C. O. Dyrby, E. J. Alexander, and T. P. Andriacchi, "Mechanical loads at the knee joint during deep flexion," *Journal of Orthopaedic Research*, vol. 20, no. 4, pp. 881–886, 2002.

[15] G. Li, S. Zayontz, L. E. DeFrate, E. Most, J. F. Suggs, and H. E. Rubash, "Kinematics of the knee at high flexion angles: an in vitro investigation," *Journal of Orthopaedic Research*, vol. 22, no. 1, pp. 90–95, 2004.

[16] K. Kanekasu, S. A. Banks, S. Honjo, O. Nakata, and H. Kato, "Fluoroscopic analysis of knee arthroplasty kinematics during deep flexion kneeling," *The Journal of arthroplasty*, vol. 19, no. 8, pp. 998–1003, 2004.

[17] G. A. Engh, R. L. Zimmerman, N. L. Parks, and C. A. Engh, "Analysis of wear in retrieved mobile and fixed bearing knee inserts," *Journal of Arthroplasty*, vol. 24, no. 6, pp. 28–32, 2009.

Hindawi Publishing Corporation
The Scientific World Journal
Volume 2014, Article ID 321080, 14 pages
http://dx.doi.org/10.1155/2014/321080

Research Article

Modelling and Analysis on Biomechanical Dynamic Characteristics of Knee Flexion Movement under Squatting

Jianping Wang,[1] Kun Tao,[2] Huanyi Li,[3] and Chengtao Wang[4]

[1] *School of Mechanical Engineering, Henan Polytechnic University, Jiaozuo 454003, China*
[2] *Department of Orthopedics, Shanghai 10th People's Hospital, Tongji University School of Medicine, Shanghai 200072, China*
[3] *Department of Orthopedics, Zhenjiang Jinshan Hospital, Zhenjiang 212001, China*
[4] *School of Mechanical Engineering, Shanghai Jiao Tong University, Shanghai 200240, China*

Correspondence should be addressed to Chengtao Wang; sjtuerwang@126.com

Received 4 January 2014; Accepted 10 February 2014; Published 11 June 2014

Academic Editors: S. Hirokawa and B. Mody

The model of three-dimensional (3D) geometric knee was built, which included femoral-tibial, patellofemoral articulations and the bone and soft tissues. Dynamic finite element (FE) model of knee was developed to simulate both the kinematics and the internal stresses during knee flexion. The biomechanical experimental system of knee was built to simulate knee squatting using cadaver knees. The flexion motion and dynamic contact characteristics of knee were analyzed, and verified by comparing with the data from in vitro experiment. The results showed that the established dynamic FE models of knee are capable of predicting kinematics and the contact stresses during flexion, and could be an efficient tool for the analysis of total knee replacement (TKR) and knee prosthesis design.

1. Introduction

All kinds of movements of the knee joint are harmonious in each joint. Due to the complicated structure and large quantity of motion, its noneffective rate in all the joints is on top. The success rate of artificial joint replacement surgery has reached 90% [1]. Even so, there were functional failure, prosthesis loosening or dislocation and the excessive wear of prosthesis, and so forth, postoperatively [2, 3]. The main factors for operation failure, in addition to the pathological reasons, come from operative and prosthetic aspects. However, the disease prevention of human knee, the design of artificial knee prosthesis, and the improvement of surgical technique depended on the research into the movement, stress, and such biomechanical characteristics about natural and artificial knee joint [4].

The internal joint contact stress and distribution of natural and artificial knee joint are directly related to its functional activities. It becomes more important to analyze the biomechanical characteristics of the motion and stress during high flexion activities [5], especially significant for population groups where lifestyle and work activities or religious activities demand deep flexion such as squatting and kneeling. However, the corresponding measurement and prediction are relatively difficult because of the limitation of ethic and measuring devices. So far, there were few effective methods to directly measure the internal stress and distribution for in vivo knee. Therefore, establishing the knee joint calculation model becomes a widely used method for predicting the internal stress and distribution. Among them, the dynamic finite element analysis has been developed into an effective method to predict the internal stress and distribution under dynamic loading conditions [6–9]. In previous models, relatively small range of flexion was conducted, usually not more than 120 degrees; there were less finite element models which can simultaneously proceed with dynamic synchronous prediction for the patellofemoral joint and femorotibial joint [7], and less have represented the whole joint with physiological soft tissue constraint [10].

In this paper, the anatomical model of three-dimensional geometric natural knee was reconstructed. Dynamic finite element (FE) model of natural knee joint, which includes

tibiofemoral, patellofemoral articulations and the surrounding soft tissues, was developed in this research, to simulate both the kinematics and internal stress during knee flexion. The biomechanical experimental system of knee flexion motion was set up to simulate human knee squatting using cadaver knees. The flexion motion and dynamic contact characteristics of knee joint were analyzed and were verified by comparison with the data from cadaver in vitro experiment.

2. Materials and Methods

2.1. Dynamic FE Knee Model

2.1.1. The Modeling of Geometric Knee. The knee of a healthy volunteer (height 1.73 m, weight 60 kg, male) had been scanned by CT (computed tomography) and MRI (magnetic resonance imaging), respectively. Then the simulation models of the knee joint bone and soft tissues were reconstructed, respectively. Due to the errors of reconstruction leading to the errors of measurement and calculation of motion, the research of precision of cortical bone reconstruction had been carried out [11]. However, the extraction of CT and MRI data was in different coordinates. It could not be directly obtained for geometric anatomic model of knee, which includes both bone and soft tissue. Bone's point cloud contour with clear geometric feature point can be cached through the MRI, so the principle of three-dimensional image registration [12] was adopted to register the point cloud contour obtained by MRI and the bone tissue profile obtained by CT. Then, a complete geometry simulation model of knee joint was built by registration of soft and bone tissues (Figure 1). The methodology and models used in this work were described thoroughly by Wang et al. (2009) [13].

2.1.2. The FE Model of Knee. Based on the above anatomical model, the mesh model of natural knee was established, which includes both bone and soft tissues, such as cartilage, meniscus, anterior and posterior cruciate ligament, medial and lateral collateral ligaments, and patellar tendon (Figure 2). The hexahedron units were adopted in all bone and soft tissues of knee FE model to reduce calculation cost. The methodology and models used in this work were described thoroughly by Wang et al. (2009) [14].

There are different features of each tissue's material properties. The material properties of the different tissues derived from literatures facilitate comparison with them. For MCL and LCL, it is an average constant from Gardiner et al. (2001) [15]. For ACL, it is single axial stress strain curve from Butler et al. (1980) [16]. For cruciate ligament and patellar tendon, it was from Suggs et al. (2008) [17]. The meniscus can be regarded as elastic and isotropic in axial, radial, and circumferential direction, respectively [18]. In this paper, the meniscus material parameters were from LeRoux and Setton (2002) [19].

Load and boundary conditions, for the FE model of natural knee, were consistent with the experimental conditions. The value of 400 N was applied to the quadriceps, which was parallel to the femur shaft and directed to the starting point of quadriceps. The value of 300 N force was applied along with the knee joint force line to simulate the weight of body [20]. Under the control of the applied muscles force, the femur move is relative to the tibia with full freedom. The movement of tibia was not active and it was *determined* by the loading conditions distributed in knee model. Nine surface contact pairs were defined for the femur, tibia, patella, and other soft tissue.

2.2. Experimental Verification. Six male volunteers' lower limb specimens were mounted into the specially designed loading and connecting device, which were connected with the standard material testing machine (CSS-44010, Changchun Research Institute for Testing machines Co., Ltd, China). This measurement system was adopted to measure both the dynamic movement and contact stress of both the tibiofemoral and the patellofemoral joints (Figure 3).

2.2.1. Experimental Devices. To realize simulation of squat movement and force loading, loading and connecting mechanisms were designed connected with the tension/compression testing machine, based on the biomechanical and boundary conditions of FEA. Accompanying squatting, three sets of measuring system were used to measure *synchronously* the relative motion and the stress of tibiofemoral and patellofemoral joint, realizing force control and loading. Experimental devices were composed of devices of loading and connective devices and the tension/compression testing machine. The loading and connective devices were designed to connect the lower limbs of cadavers and tension/compression testing machine, loading the gravity and quadriceps force to realize joint flexion, which were composed of the upper and the lower connection device (Figure 4). The cadaver knee's dynamic translation and rotation (and lock) in coronal, sagittal, and cross sectional planes can be implemented, simulating living knee movement.

Optical tracking system (Polaris hybrid optical tracking system, NDI, Calgary, AB, Canada) was used to measure the trajectory of the femur, tibia, and patella under squatting for analysis of knee relative motion by coordinate transformation [21] (Figure 5). Coordinate system was established by measuring knee's bone marker points, and knee joint rotations were defined according to the clinical joint coordinate system (JCS) [22, 23]. The same method was used for FE model.

Tecscan measurement system (Tescan Inc., Boston, MA, USA) was used to implement contact measurement (Figure 6). The measurement system is comprised of I-scan sensor, data conversion handle, data analysis, and calibration software. The special sensor I-scan 4000 was used for tibiofemoral joint. This sensor consists of two pieces of separate sensors, whose specifications are of 33 mm $*$ 28 mm, 0.1 mm thick. The I-scan 5051 sensor was used for patellofemoral joint's contact measurement [24]. In the experiments, the articular capsule was opened, and then the sensing piece of I-scan sensor was, respectively, put into the joint gaps of tibiofemoral and patellofemoral joint (Figure 7).

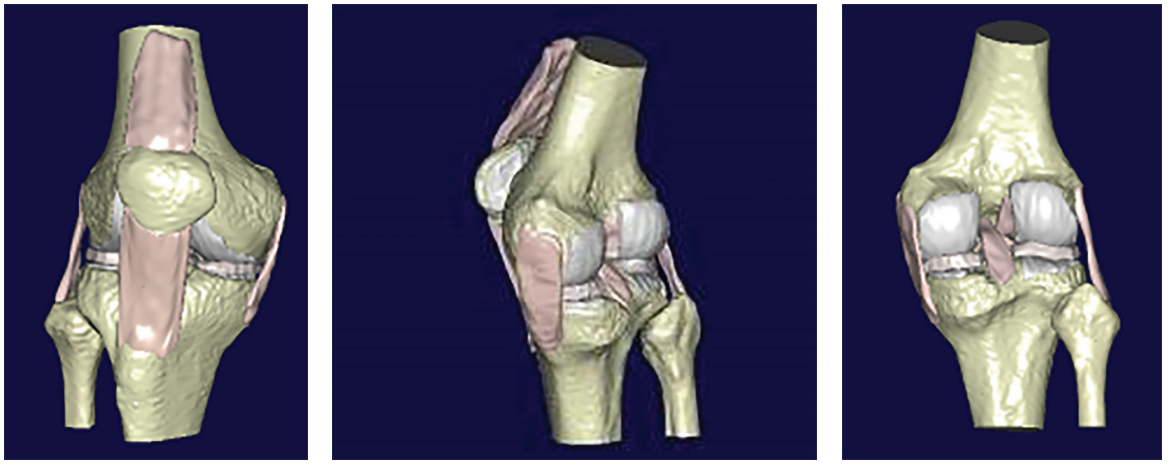

(a) (b) (c)

Figure 1: The geometric anatomy model of human knee.

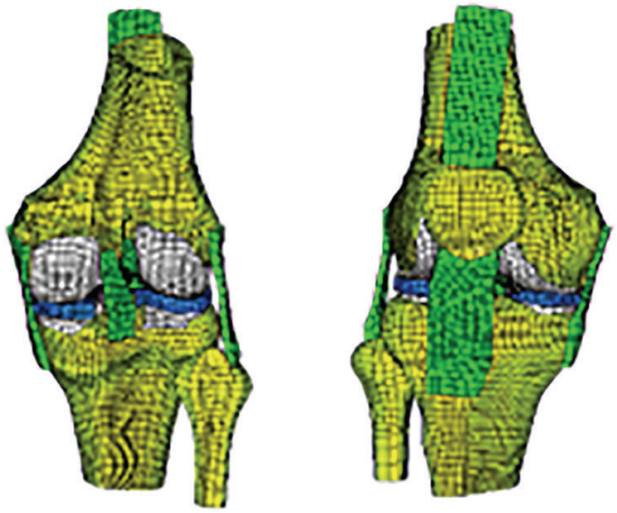

(a) (b)

Figure 2: The FE model of knee.

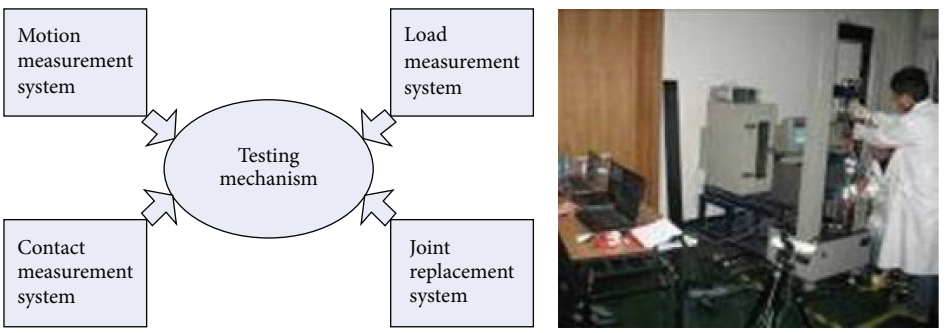

(a) (b)

Figure 3: The flowchart and the real of knee experiment system.

(a)

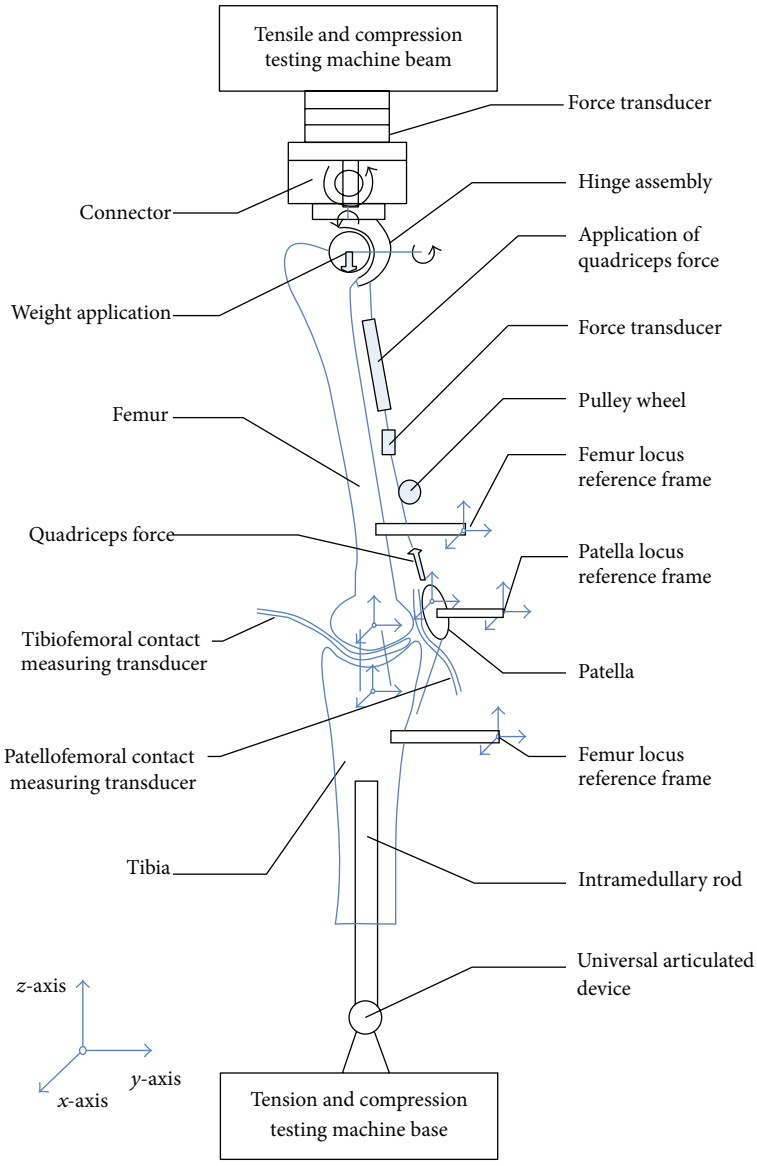

(b)

Figure 4: Setup of knee experiment.

The gravity loading of the femoral head was controlled and *measured* by the sensor on the mobile beam of tension/compression testing machine. The quadriceps force and connection test device was connected to the force sensor CFBLS-25 (25 Kg maximum load, 0.03% FS, Shanghai Yichuan Instrument Factory) and the amplifier VM641 (±0.1% accuracy, Guangzhou Huamao Sensor Co., Ltd.). The sensor, pulley, and screw were connected to form loading and measuring device, which was used to measure and control the tension of quadriceps. The output signal of the amplifier was collected by the DAQ Card (data acquisition card) (Yanhua PCI-1710L, Advantech Co., Ltd.). And the measured results were outputted by the commercial software Labview (Laboratory Virtual Instrumentation Engineering Workbench, United States National Instruments Company).

2.2.2. Experimental Loading and Measurement. The I-scan 4000 and the I-scan 5051 pressure test pieces were placed, respectively, in tibiofemoral and patellofemoral joint, and the articular capsule was sutured. The specimen was fixed into the experimental platform. The gravity loading on the femoral head was controlled and measured by sensor of tension/compression testing machine. The tension of quadriceps tendon was outputted by the DAQ Card and the commercial software Labview. Simultaneously, the contact pressure of tibiofemoral joint was recorded by the I-scan contact measurement system. For dynamic movement measurement, three reference frames consisting of 14 mm diameter markers were fixed in tibia, femur, and patella, respectively. The data of markers were captured and the relative motions of patella,

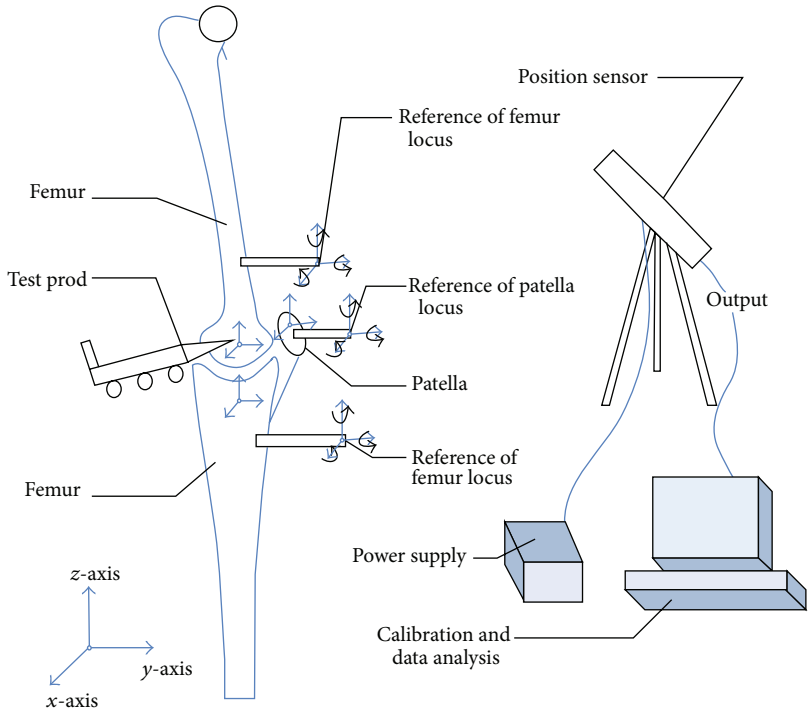

Figure 5: The measurement system of movement.

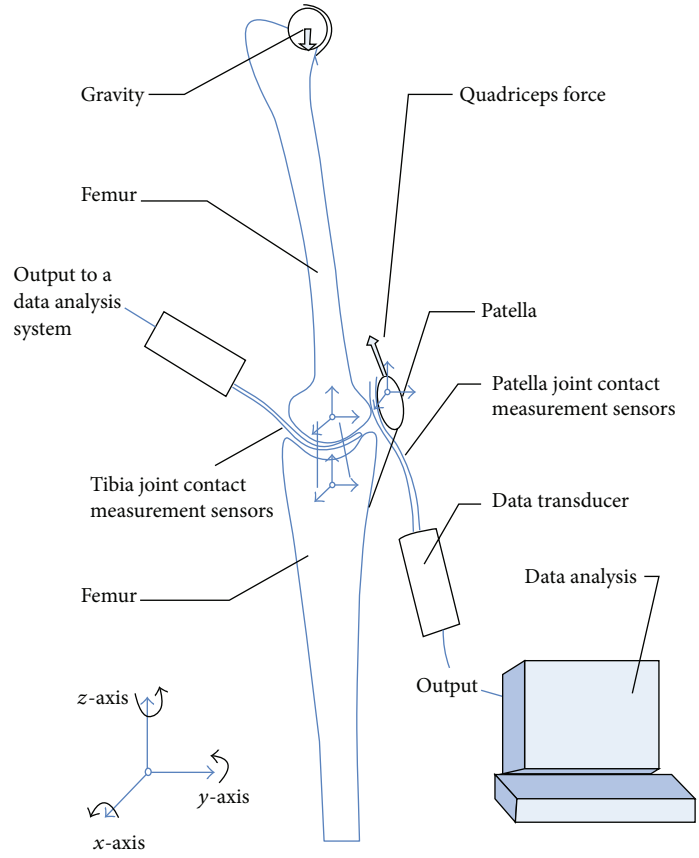

Figure 6: The measurement system of contact.

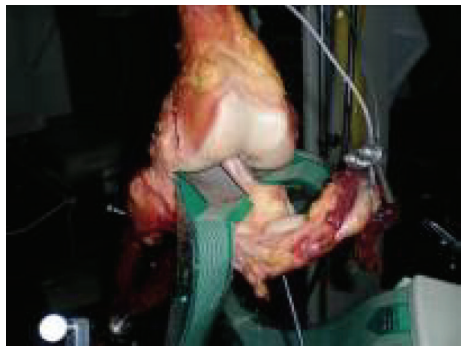

Figure 7: The location of Tecscan sensor.

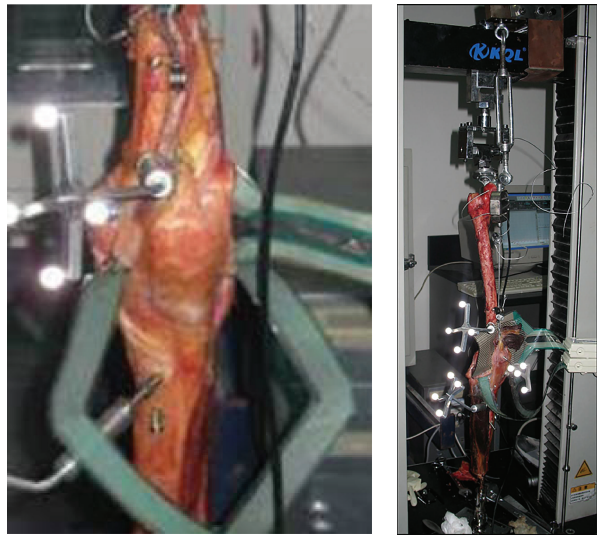

(a) (b)

Figure 8: The device after installation.

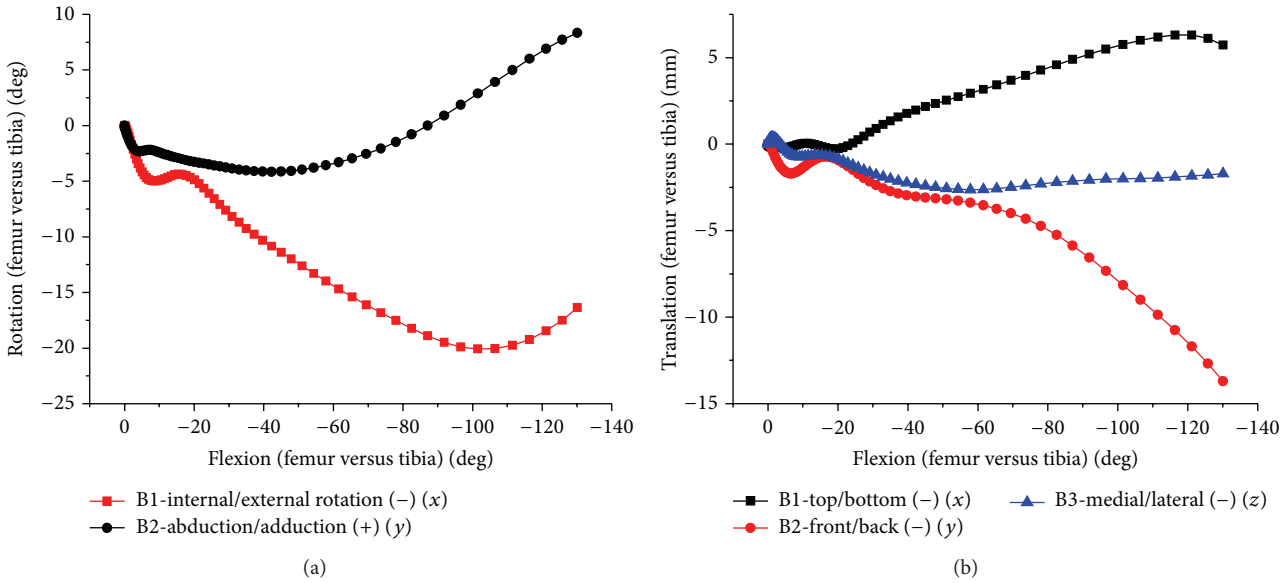

Figure 9: The relative movement of natural tibiofemoral joint. (a) Internal/external and abduction/adduction of tibiofemoral joint. (b) Translation of tibiofemoral joint.

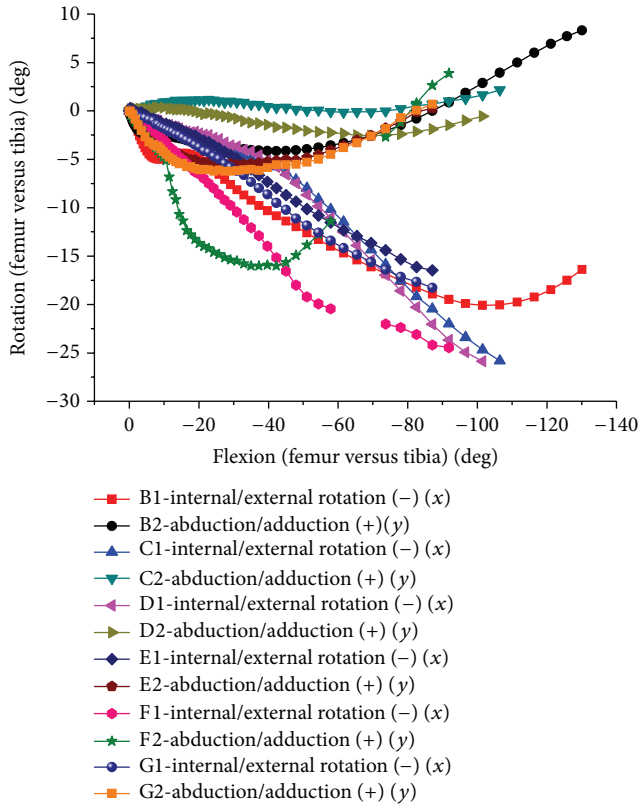

Figure 10: Internal/external and abduction/adduction of tibiofemoral joint relative movements in both test and FEA.

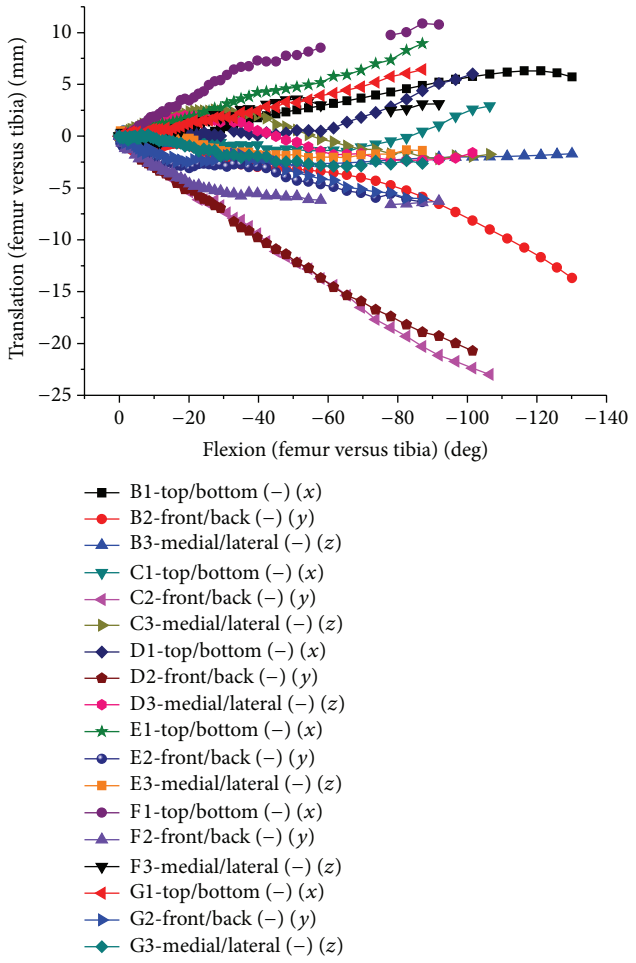

Figure 11: The relative translation of tibiofemoral joint in both test and FEA.

tibia, and femur were measured by the Polaris optical tracking system (Figure 8).

3. Results

3.1. The FE Calculation and Experimental Results of Knee Joint. The FE model was developed into the software of ABAQUS-6.5.1 (HKS, Pawtucket, RI) to analyze the articular contact and the relative motion of the patellofemoral joint and tibiofemoral joint synchronously. By calculating the dynamic FEA of natural knee, the movement and joint contact stress of healthy knee could be obtained. The flexion motion and dynamic contact characteristics of knee joint were analyzed and verified by comparison with the data from cadaver in vitro experiment.

3.1.1. The FE Results and Verification Analysis of Tibiofemoral Joint. The tibial internal rotation increases as knee flexes, and femoral relative external rotation decreases after about 90° flexion, accompanying 9° adduction of femur (Figure 9). The femur backward translation increased along with knee flexing. In high flexion, femoral condyle lifted off tibial surface a few millimeters and contacted with posterior meniscus. Smaller medial-lateral translation happened in the entire flexion. The cadaver experiment and FE results were compared in contrast diagram (Figures 10 and 11).

During 0–90-degree knees flexion, femur external rotation was average of 20 degrees, and femur abduction turned to average of 2 degrees. From 90–120-degree flexion, the tibial internal rotation increased while femur external rotation decreased. Synchronously, the femoral adduction increased. There was unusual abduction for one of the specimens during earlier flexion stage. The femur translation trends of the experiment and FE results were basically consistent (Figure 11) in the direction of medial-lateral, up-down, and front-back, respectively. With flexion growth, femoral relative tibial translated upward, inward and backward, respectively. Two cases translated downward within 20–70-degree flexion. The backward translation was relatively small, which was approximately 7 mm at 90-degree flexion, being similar to simulation results. There was a large backward translation for one case, approximately 23 mm around 110-degree flexion. There was bigger difference for translation result, which may be caused by the error of selecting the osseous marker points and the individual difference.

With knee flexion from 0 to 130 degrees, the average peak stress of tibiofemoral joint was 10 MPa at 0 degrees and 6 MPa at 30~90 degrees, and it increased to 21 MPa

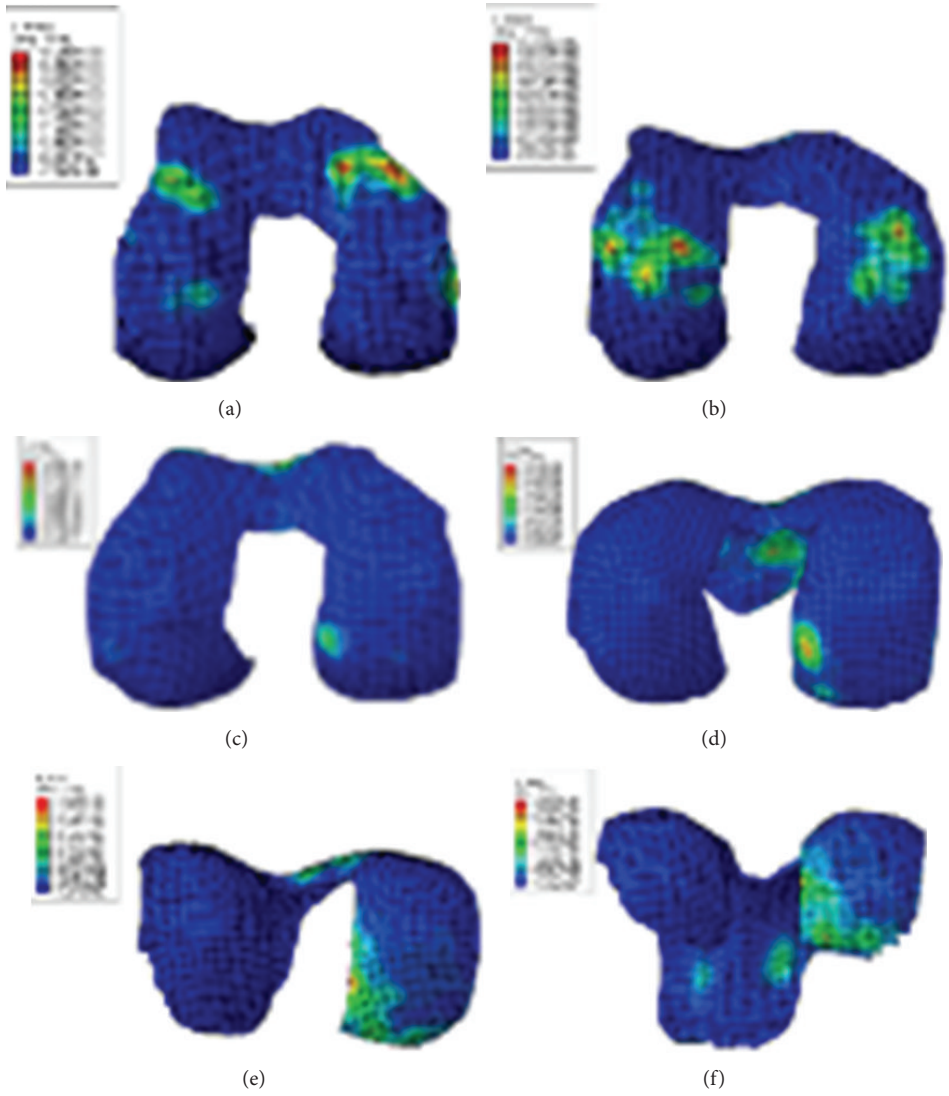

Figure 12: Contact stress of 0-30-60-90-130 degree flexion of tibiofemoral joint in FEA. (a) Stress distribution of 0° flexion. (b) Stress distribution of 30° flexion. (c) Stress distribution of 60° flexion. (d) Stress distribution of 90° flexion. (e) Stress distribution of 120° flexion. (f) Stress distribution of 130° flexion.

from 90 to 130 degrees. There were differences between the medial and the lateral tibiofemoral joint. From 0- to 60-degree flexion, medial and lateral contact stresses were close for FE results, but the lateral contact stress was higher than the medial contact stress for in vitro test. Starting from 90-degree flexion, larger contact stress was in the medial tibiofemoral joint for both of FE and in vitro test. Simultaneously, in the lateral tibiofemoral joint, there was little contact for FE results and about 4 MPa small contact stress for in vitro test. In 0–30-degree flexion, the contact of tibiofemoral joint mainly occurred in the front of tibia, and contact area was relatively small. Within 30~60-degree flexion, contact was mainly in the central tibia; contact area is increasing and causing smaller contact stress. With flexion deepening, the backward translation of femur increased, contacting with the posterior meniscus, and lateral femoral condyle lift off tibial surface a few millimeters in higher flexion (Figures 12 and 13). Accordingly, the total contact area of tibiofemoral joint relatively decreased, causing larger contact stress in the medial tibiofemoral joint.

3.1.2. The FE Results and Verification Analysis of Patellofemoral Joint. With flexion of tibiofemoral joint, the flexion change of patellofemoral joint was basically linear (Figure 14). Accompanying patella's small angle external rotation and medial tilting relative to femur, there were small medial, backward, and upward translations. Patella was up to about 90 degrees flexion, external rotation of 3.7 degrees, medial tilting of 10 degrees, backward translation of 64 mm, the maximum downward translation of 49 mm at about 90 degrees knee flexion, and the maximum lateral translation of 6 mm at about 80 degrees knee flexion.

The change tendency was basically consistent in simulation and test (Figures 15 and 16), being slightly different.

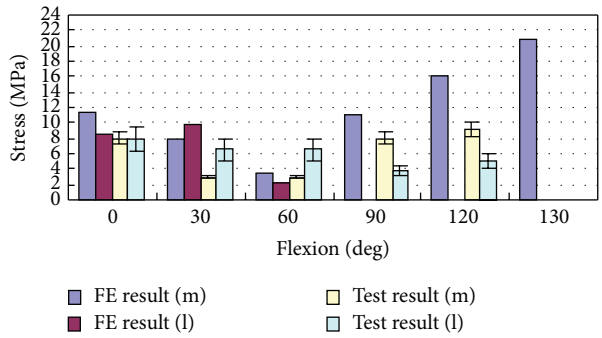

Figure 13: Comparison between experimentally measured stress applied to tibiofemoral joint and the FE results, where m refers to the medial femur and l refers to the lateral femur.

The patella internal rotation (20 degrees maximum) was bigger than simulation results. There was little difference for patella relative medial tilting, excepting lateral tilting at 60 degrees flexion in one case. It was basically consistent in relative flexion of patellas, being linear with tibiofemoral flexion. The fluctuations of translation were larger than the rotation. The maximum medial translation in the experiment occurred within 30 degrees flexion earlier than the simulation of about 70 degrees flexion. However, the upward and backward translations were larger than the simulation. This difference may be caused by soft tissue relaxation in the cadaver experiment.

With knee flexion, the contact place of patellofemoral joint gradually moved from the inferior patella to the superior patella and then turned slightly downward after 120 degrees. Within 30 degrees of flexion, the contact places of patellofemoral joint were unsteady. Within 30–90 degrees, the contact places of patellofemoral joint gradually drifted to the medial and lateral patella; the contact places were mainly on the medial patella ridge. Starting from 90-degree flexion, contact position was obviously distributed in medial and lateral margin patella. From 0- to 90-degree flexion, the contact stress was of about 9 MPa for both the simulation and the test results. The medial contact stress was significantly greater than the lateral one except within 30-degree flexion. The contact stress increased after 90°, reaching 22 MPa at 130-degree flexion. The margin patella contacted with femoral epicondylus in higher flexion and decreased contact area causing higher contact stress (Figures 17 and 18).

4. Discussion

4.1. The Experimental System Analysis. To fully understand the function of knee joint, not only the synchronal measurement of both tibiofemoral and patellofemoral articulations but also the synchronal measurement of both kinematics and contact can be implemented in this experiment system and simulation. Because of the difficulty of accurately measuring internal joint contact stress in rational functional conditions, there was seldom contact research about the tibiofemoral joint. Hsu et al. (1997) [25] used unidirectional sensor embedded in patellar prosthesis to measure patellofemoral joint contact force. And it was limited that the force and movement were measured separately. Powers et al. (1998) [26] used electromagnetic tracking equipment to measure the patella movement and used pressure sensitive film to measure patellofemoral joint contact pressure and area. However, tibiofemoral joint was not measured. Halloran et al. (2010) [9] developed a whole joint model, and this included fixture components only. Prior work with cadaveric specimens included displacement control of TF kinematics and only PF soft tissue representations [27].

The in vitro experiment and simulation results were compared in this study, and there were differences between them. The accuracy of test was inevitably influenced by some of the characteristics of experiment system. Although the thickness of sensing piece is only 0.1 mm, the joint surface shape was slightly changed, and the results accuracy of contact area and contact pressure peak in joint was affected. The difference of reference point selection caused the difference of coordinate system, which led to measurement error of movement. Due to the limitation of measurement mechanism itself, it is difficult to perfectly simulate the human knee joint squat movement. In vitro test research showed that quadriceps force size and loading direction influence tibiofemoral joint rotation, especially within 0~90 degrees flexion; the force and angle (Q angle) reduction of quadriceps caused tibial internal rotation reduction [28, 29]. Therefore, the difference between simulation and living quadriceps activities may be one of the reasons of the tibial rotation difference between in vitro and living tests. The signal interference of sensor, measurement errors of force transducer, contact stress sensor, reference frame, and calibration error can also cause measurement error. Because of losing activity, the muscles and joints of specimens will be stiff, and decreased joint fluid lubrication in articular capsule increased joint contact friction. And the mechanical property of bone and soft tissue changed accompanied with relaxing and drying of specimen organization itself. These conditions may all affect the experimental results. So there are differences between the simulation and the results of the experiment, as well as between the specimen and living body. In addition, individual differences can also cause difference. Therefore, the experimental method also needed to be continuously developed to improve the biomechanical research of knee.

4.2. Natural Human Knee Flexion Biomechanical Analysis. Along with the knee flexion, natural knee joint femur rolled backward and tibia internally rotated. The results of movement of femur relative tibia were basically consistent with Iwaki (2000) and Johal et al. (2005) [30, 31]. Within 0- to 30-degree flexion, tibial internal rotation increased (3.3–12.8 degrees). Within 30~90-degree flexion, natural knee tibial rotation was bigger (10.6–17.5), maintaining internal rotation, which is approximate to previous results of passive flexion with no loading (25-degree internal rotation at 100-degree passive flexion) [32]. And it was different from Hirokawa et al. (1992) [29] (1-degree external rotation at 120-degree flexion) and Van Kampen and Husikes (1990) [33] (internal rotation began until 120-degree flexion for three of the four specimens, in which fixed femoral test equipment was used). If rotating force was applied on tibia, especially for the unloading knee,

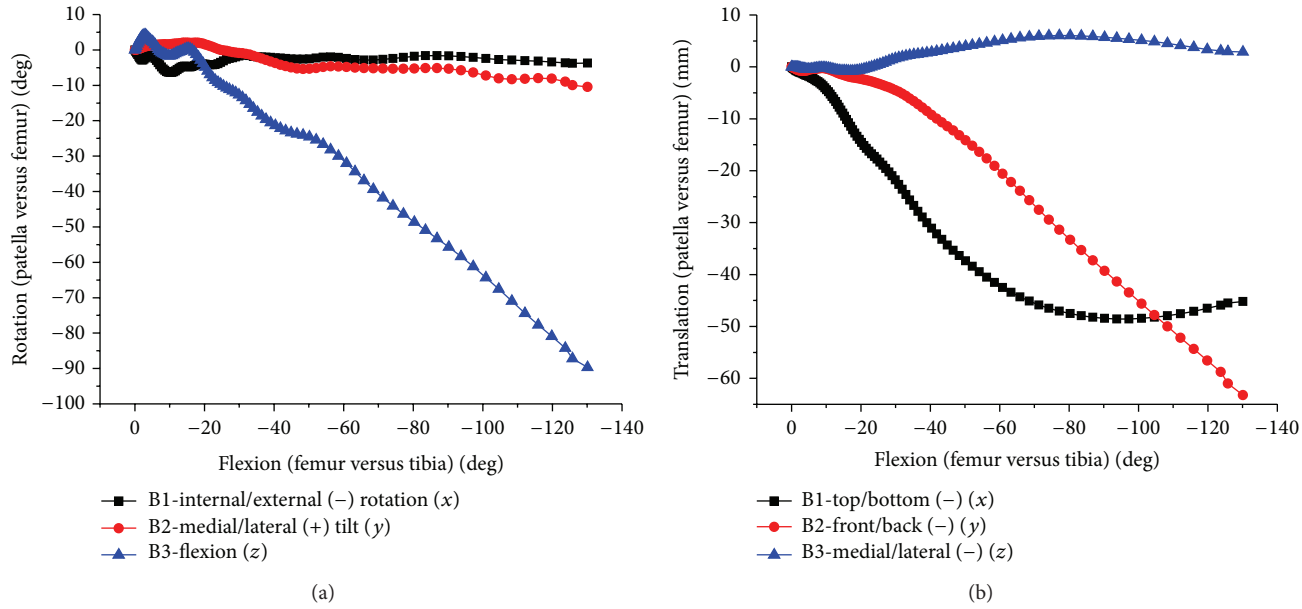

FIGURE 14: The relative movement of patellofemoral joint. (a) Internal/external, abduction/adduction, and flexion of patellofemoral joint. (b) Translation of patellofemoral joint.

femur external rotation at 90 degree is reversible. Therefore, if the tibia flexes 90 degrees at external rotation phase, it is possible to stretch to 20-degree flexion with no lateral condyle backward-forward translation. So, to great extent, the tibia rotation belongs to tibial rotation belong to "combining" not inevitable within 20~90 degrees flexion. However, the 20-degree flexed position was the critical point of tibia in internal rotation. Therefore, tibia internal rotation was inevitable within 0~20 degrees flexion, rotating around the long axis of knee.

The results of knee adduction-abduction about living body were little reported recently. The research in this paper showed that the femoral external rotation was along with the adduction. The reason is that the medial tibia platform is more concave than the lateral one and the projection on coronal plane of medial condyle is lower than that of the lateral condyle [34]. No eversion in knee flexion due to the consistent curvature radius of the medial and lateral femoral posterior condyle, no distal outstanding of medial condyle. The adduction in higher flexion was caused and corresponded with the internal rotation of tibia relative to femur. The research results of Hsieh et al. (1998) [35] (0-degree adduction at 90-degree flexion) and Kurosawa et al. (1985) [36] (2.2-degree adduction at 120-degree flexion) were within the scope of this study.

Within hol-extension to passive flexion (more than 120-degree flexion), there was 10 mm femoral condylar backward rolling. Femoral condyle scrolled up to meniscus posterior horn, almost dislocation to the tibia. This result is consistent with Nakagawa et al. (2000) [37] of no loading deep flexion Japan knee and Abdel-Rahman and Hefzy (1998) [38] ray research results. Wilson et al. (2000) [32] research results were of 24 ± 4 mm backward translation, 13 ± 4 mm distal translation, and 5 ± 3 mm medial translation after 100-degree flexion, which were approximate to this paper. Wretenberg et al. (2002) [39] analyzed 16 nonload right tibiofemoral joint contact at 0-degree, 30-degree, and 60-degree flexion by MRI and observed that the lateral displacement was bigger than the medial. The research of Johal et al. (2005) [31] showed that femoral condyle translated backward within 0~90-degree flexion, accompanied with slipping or rolling.

In this study, the distribution of medial and lateral contact stress was influenced by the joint position. The peak stress of tibiofemoral joint contact was of average 10 MPa at 0-degree flexion and 6 MPa within 30~90-degree flexion, and it grew from 90-degree flexion reaching 21 MPa at 130-degree flexion. In the flexion process, the medial and lateral tibiofemoral joint contact stresses were different. From 0- to 60-degree flexion, medial stress was approximate to the lateral stress for FEA and slightly larger contact stress at lateral joint for in vitro experiment. Within 0~30-degree flexion, contact position was mainly in anterior tibia, and contact area was relatively small. From 30- to 60-degree flexion, the contact mainly occurred in central tibia, increased contact area, and decreased contact stress. Along with deepening flexion, femur backward translation and liftoff increased, which decreased tibiofemoral articular contact area. After 90-degree flexion, larger contact stress occurred in medial joint for FEA and in vitro experiment. The 21 MPa maximum contact stress of simulation analysis results was closed to 25 MPa cartilage cracking limitation [40] (Torzilli et al., 1999), being consistent with Ashvin Thambyah et al. (2005) [5] which is of 14 MPa average stress peak (standard deviation 2.5 MPa) on walking phase. The loaded living research by Iwaki et al. (2000) and Hill et al. (2000) [30, 41] showed that large change occurred in high flexion for tibiofemoral joint, and too much stress (more than 25 MPa) caused cartilage injury, which may be the cause of the continued development

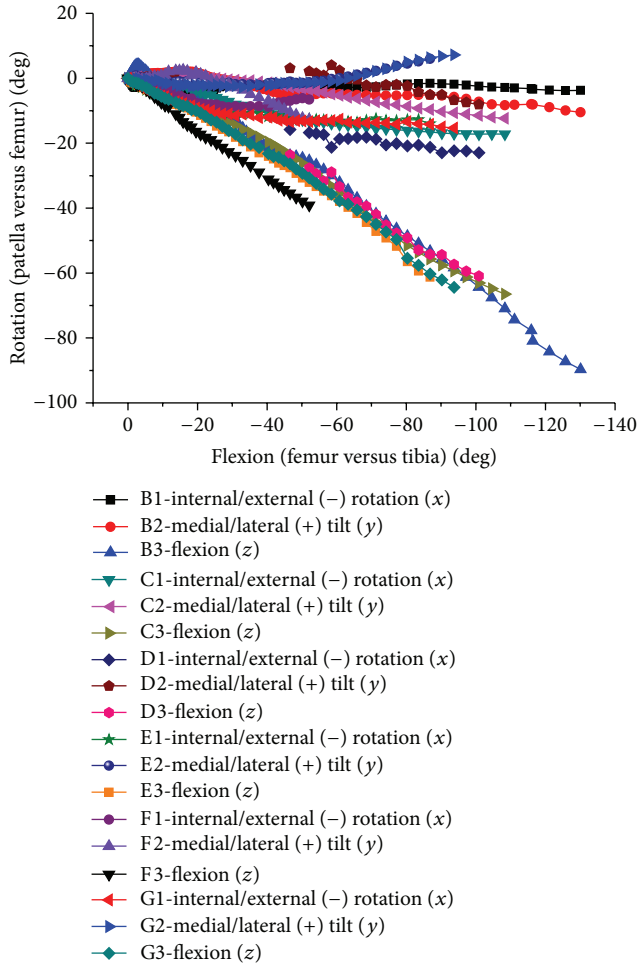

Figure 15: Internal/external, abduction/adduction, and flexion of patellofemoral joint relative movements in both test and FEA.

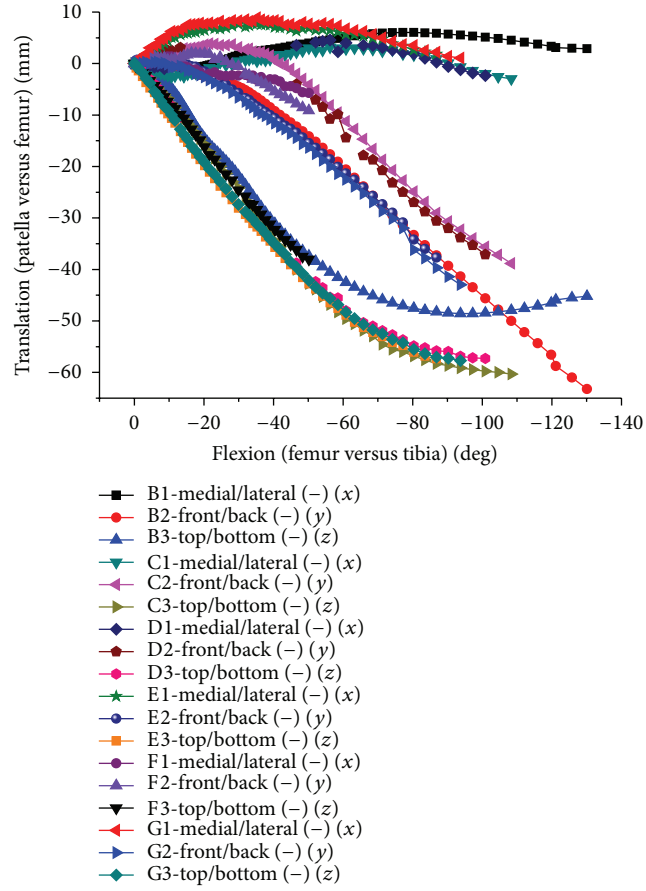

Figure 16: Translation of patellofemoral joint relative movement in both test and FEA.

of joint degeneration. Contact area reduction within high flexion was likely the reason of high stress in high flexion, and the cause of high stress was not only from high loading.

In lateral knee joint, considerable backward translation occurred, accompanied femur lifting off the lateral tibia and fall on the posterior horn of meniscus, the femur being subluxation. At the same time medial stress increased, which may be the reason of medial meniscus tear.

As for patellofemoral joint movement, Zavatsky et al. (2004) [42] gave the measurement result, and it is consistent with this research. Even though there are different reference points and reference frames, the calculation and measurement of patellofemoral relative rotation in this paper were within the standard deviation range being consistent with other research [35]. The patellofemoral joint translation motion results (backward, distal, medial, or lateral translation) also were approximate to other results [25, 33, 35]. At the same time, patellofemoral flexion was lagged behind the tibiofemoral flexion, which was consistent with the relative reports [33, 35, 43].

The contact point's upward movement of the healthy patellofemoral joint mainly occurred in early flexion, which was consistent with the previous in vitro [44, 45] and in vivo research [46]. The data of this study showed that, after 60-degree flexion, the contact area was relatively stable in the proximal portion of patella and symmetrically distributed in medial and lateral patellar surface, with no contact near the ridge of the patella. The research of Suzuki et al. (2012) [47] was approximate to this paper. And patellofemoral contact area increased with the knee flexion, of 70% average growth within 30 degrees flexion and of 34% average increase within 30~60 degrees flexion [48]. It was also found in this research that, with the deepening tibiofemoral joint flexion, the patellar tendon resulted in medial tilting so that the patella odd facet contact with the femur reduced the tension of the patellar tendon and quadriceps. At the same time, there was always a contact zone (concave area) at the upper patella and the contact occurred in the intercondylar notch along with the medial and lateral contact, a recess located in the upper patella exactly matching with the trochlear.

In higher flexion, the curvature radius of the femoral condyles was shorter and the lateral collateral ligament and anterior cruciate ligament were slack. Meanwhile, with tibiofemoral joint flexing, the tibiofemoral joint pressure increased, and the tension of the quadriceps tendon and the patellar tendon increased. The study showed that arthritis and cartilage damage was the result of the repeated or high contact stress [49], while the medial tibiofemoral was

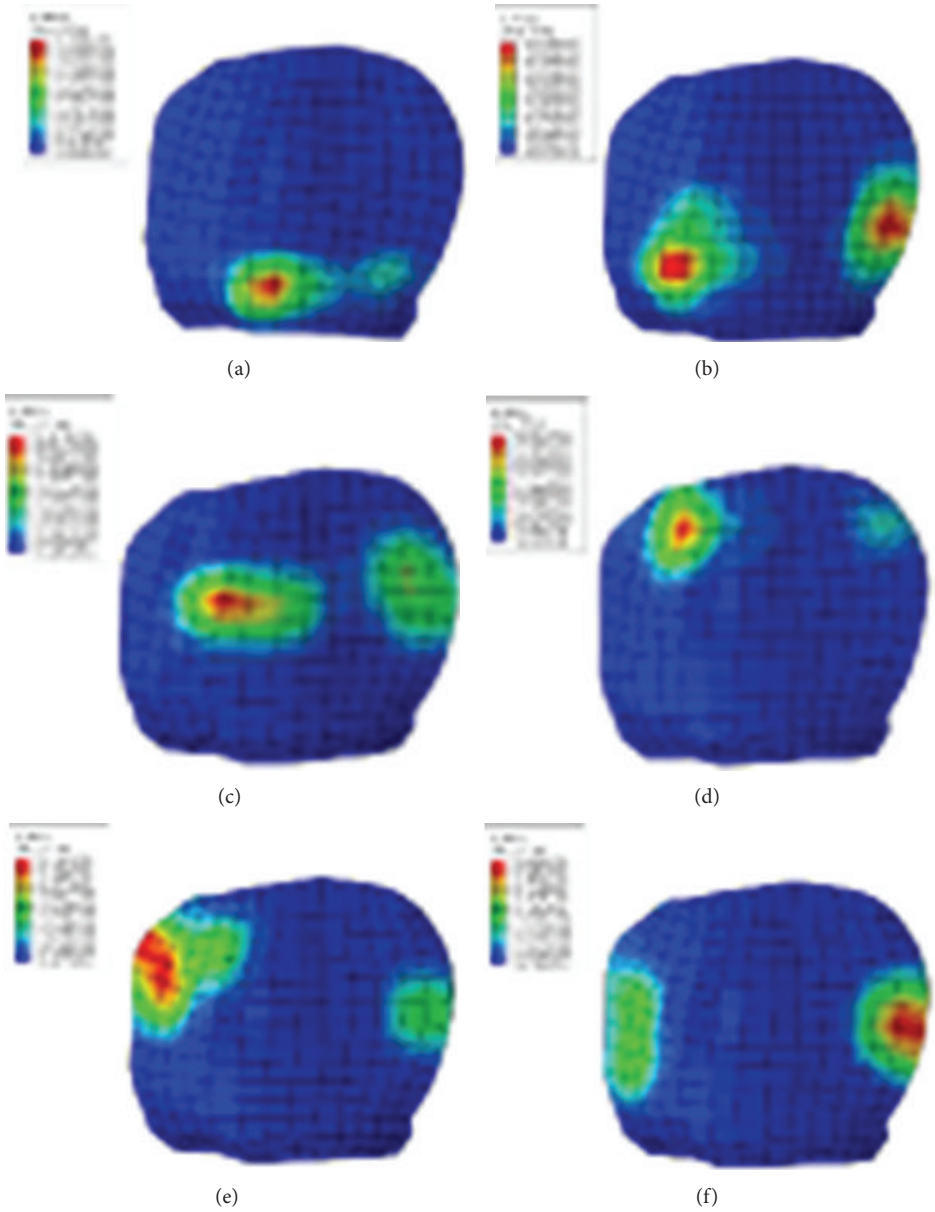

Figure 17: Contact stress of 0-30-60-90-130 degree flexion of tibiofemoral joint in FEA. (a) Stress distribution of 0° flexion. (b) Stress distribution of 30° flexion. (c) Stress distribution of 60° flexion. (d) Stress distribution of 90° flexion. (e) Stress distribution of 120° flexion. (f) Stress distribution of 130° flexion.

prone to arthritis, leading to an articulated knee. There was difference between Westerners and Asians, especially in the high flexion activities [50]. Arched knee is more likely to occur in Asians. It could not be ignored for the mechanical factors causing knee disease from the activities or ethnic differences between Asians and Westerners. Especially for Asians, the relationship between mechanics and movement in high flexion should be fully understood.

Conflict of Interests

All authors contributed significantly to the study and paper preparation, and none demonstrates any conflict of interests regarding this submission.

Authors' Contribution

Jianping Wang and Kun Tao are the first authors for this paper.

Acknowledgments

This work was primarily supported by the "Research on the properties of hip and knee joints and basic design of artificial joints for Asia Race" project funded by the National Natural Science Foundation of China (30810103908). And further support was from the "Research on high-flexion stability mechanism of high-flexion artificial knee" project funded by the National Natural Science Foundation of China

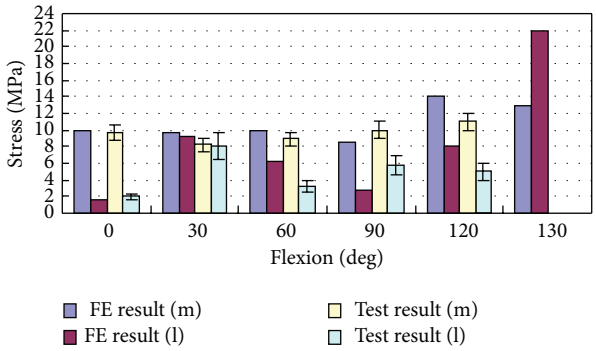

Figure 18: Comparison between experimentally measured stress applied to patella cartilage and the FE results, where m refers to the medial patella and l refers to the lateral patella.

(31370999) and National Natural Science Foundation of China (81000808).

References

[1] K. Knutson, S. Lewold, O. Robertsson, and L. Lidgren, "The Swedish knee arthroplasty register: a nation-wide study of 30,003 knees 1976–1992," *Acta Orthopaedica Scandinavica*, vol. 65, no. 4, pp. 375–386, 1994.

[2] E. Luger, S. Sathasivam, and P. S. Walker, "Inherent differences in the laxity and stability between the intact knee and total knee replacements," *Knee*, vol. 4, no. 1, pp. 7–14, 1997.

[3] G. W. Blunn, A. B. Joshi, R. J. Minns et al., "Wear in retrieved condylar knee arthroplasties: a comparison of wear in different designs of 280 retrieved condylar knee prostheses," *Journal of Arthroplasty*, vol. 12, no. 3, pp. 281–290, 1997.

[4] M. S. Hefzy and E. Abdel-Rahman, "Dynamic modeling of the human knee joint: formulation and solution techniques. a review paper," *Biomedical Engineering—Applications, Basis and Communications*, vol. 7, no. 1, pp. 5–21, 1995.

[5] A. Thambyah, J. C. H. Goh, and S. Das De, "Contact stresses in the knee joint in deep flexion," *Medical Engineering and Physics*, vol. 27, no. 4, pp. 329–335, 2005.

[6] A. C. Godest, M. Beaugonin, E. Haug, M. Taylor, and P. J. Gregson, "Simulation of a knee joint replacement during a gait cycle using explicit finite element analysis," *Journal of Biomechanics*, vol. 35, no. 2, pp. 267–275, 2002.

[7] J. P. Halloran, A. J. Petrella, and P. J. Rullkoetter, "Explicit finite element modeling of total knee replacement mechanics," *Journal of Biomechanics*, vol. 38, no. 2, pp. 323–331, 2005.

[8] C. K. Fitzpatrick and P. J. Rullkoetter, "Influence of patellofemoral articular geometry and material on mechanics of the unresurfaced patella," *Journal of Biomechanics*, vol. 45, no. 11, pp. 1909–1915, 2012.

[9] J. P. Halloran, C. W. Clary, L. P. Maletsky, M. Taylor, A. J. Petrella, and P. J. Rullkoetter, "Verification of predicted knee replacement kinematics during simulated gait in the Kansas knee simulator," *Journal of Biomechanical Engineering*, vol. 132, no. 8, Article ID 081010, 2010.

[10] M. A. Baldwin, C. W. Clary, C. K. Fitzpatrick, J. S. Deacy, L. P. Maletsky, and P. J. Rullkoetter, "Dynamic finite element knee simulation for evaluation of knee replacement mechanics," *Journal of Biomechanics*, vol. 45, no. 3, pp. 474–483, 2012.

[11] J. Wang, M. Ye, Z. Liu, and C. Wang, "Precision of cortical bone reconstruction based on 3D CT scans," *Computerized Medical Imaging and Graphics*, vol. 33, no. 3, pp. 235–241, 2009.

[12] P. J. Besl and N. D. McKay, "A method for registration of 3-D shapes," *IEEE Transactions on Pattern Analysis and Machine Intelligence*, vol. 14, no. 2, pp. 239–256, 1992.

[13] J.-P. Wang, L.-W. Qian, and C.-T. Wang, "Simulation of geometric anatomy model of human knee joint," *Journal of System Simulation*, vol. 21, no. 10, pp. 2806–2809, 2009.

[14] J. Wang, H. Wu, and Ch. Wang, "Dynamic finite ememen modeling of human knee joint and application in TKR," *Journal of Medical Biomechanics*, vol. 24, no. 5, pp. 333–337, 2009.

[15] J. C. Gardiner, J. A. Weiss, and T. D. Rosenberg, "Strain in the human medial collateral ligament during valgus loading of the knee," *Clinical Orthopaedics and Related Research*, no. 391, pp. 266–274, 2001.

[16] D. L. Butler, F. R. Noyes, and E. S. Grood, "Ligamentous restraints to anterior-posterior drawer in the human knee. A biomechanical study," *Journal of Bone and Joint Surgery A*, vol. 62, no. 2, pp. 259–270, 1980.

[17] J. F. Suggs, G. R. Hanson, S. E. Park, A. L. Moynihan, and G. Li, "Patient function after a posterior stabilizing total knee arthroplasty: cam-post engagement and knee kinematics," *Knee Surgery, Sports Traumatology, Arthroscopy*, vol. 16, no. 3, pp. 290–296, 2008.

[18] F. R. Noyes and E. S. Grood, "The strength of the anterior cruciate ligament in humans and rhesus monkeys: age related and species related changes," *Journal of Bone and Joint Surgery A*, vol. 58, no. 8, pp. 1074–1082, 1976.

[19] M. A. LeRoux and L. A. Setton, "Experimental and biphasic FEM determinations of the material properties and hydraulic permeability of the meniscus in tension," *Journal of Biomechanical Engineering*, vol. 124, no. 3, pp. 315–321, 2002.

[20] G. Li, E. Most, E. Otterberg et al., "Biomechanics of posterior-substituting total knee arthroplasty: an in vitro study," *Clinical Orthopaedics and Related Research*, no. 404, pp. 214–225, 2002.

[21] L. Klimek, U. Ecke, B. Lübben, J. Witte, and W. Mann, "A passive-marker—based optical system for computer-aided surgery in otorhinolaryngology: development and first clinical experiences," *Laryngoscope*, vol. 109, no. 9, pp. 1509–1515, 1999.

[22] E. S. Grood and W. J. Suntay, "A joint coordinate system for the clinical description of three-dimensional motions: application to the knee," *Journal of Biomechanical Engineering*, vol. 105, no. 2, pp. 136–144, 1983.

[23] G. K. Cole, B. M. Nigg, J. L. Ronsky, and M. R. Yeadon, "Application of the joint coordinate system to three-dimensional joint attitude and movement representation: a standardization proposal," *Journal of Biomechanical Engineering*, vol. 115, no. 4, pp. 344–349, 1993.

[24] M. L. Harris, P. Morberg, W. J. M. Bruce, and W. R. Walsh, "An improved method for measuring tibiofemoral contact areas in total knee arthroplasty: a comparison of K-scan sensor and Fuji film," *Journal of Biomechanics*, vol. 32, no. 9, pp. 951–958, 1999.

[25] H.-C. Hsu, Z.-P. Luo, J. A. Rand, and K.-N. An, "Influence of lateral release on patellar tracking and patellofemoral contact characteristics after total knee arthroplasty," *Journal of Arthroplasty*, vol. 12, no. 1, pp. 74–83, 1997.

[26] C. M. Powers, J. C. Lilley, and T. Q. Lee, "The effects of axial and multi-plane loading of the extensor mechanism on the patellofemoral joint," *Clinical Biomechanics*, vol. 13, no. 8, pp. 616–624, 1998.

[27] M. A. Baldwin, C. Clary, L. P. Maletsky, and P. J. Rullkoetter, "Verification of predicted specimen-specific natural and implanted patellofemoral kinematics during simulated deep knee bend," *Journal of Biomechanics*, vol. 42, no. 14, pp. 2341–2348, 2009.

[28] S. C. Shoemaker, D. Adams, D. M. Daniel, and S. L. Woo, "Quadriceps/anterior cruciate graft interaction: an in vitro study of joint kinematics and anterior cruciate ligament graft tension," *Clinical Orthopaedics and Related Research*, no. 294, pp. 379–390, 1993.

[29] S. Hirokawa, M. Solomonow, Y. Lu, Z.-P. Lou, and R. D'Ambrosia, "Anterior-posterior and rotational displacement of the tibia elicited by quadriceps contraction," *The American Journal of Sports Medicine*, vol. 20, no. 3, pp. 299–306, 1992.

[30] H. Iwaki, V. Pinskerova, and M. A. R. Freeman, "Tibiofemoral movement 1: the shape and relative movements of the femur and tibia in the unloaded cadaver knee," *Journal of Bone and Joint Surgery B*, vol. 82, no. 8, pp. 1189–1195, 2000.

[31] P. Johal, A. Williams, P. Wragg, D. Hunt, and W. Gedroyc, "Tibio-femoral movement in the living knee. A study of weight bearing and non-weight bearing knee kinematics using 'interventional'MRI," *Journal of Biomechanics*, vol. 38, no. 2, pp. 269–276, 2005.

[32] D. R. Wilson, J. D. Feikes, A. B. Zavatsky, and J. J. O'Connor, "The components of passive knee movement are coupled to flexion angle," *Journal of Biomechanics*, vol. 33, no. 4, pp. 465–473, 2000.

[33] A. Van Kampen and R. Husikes, "The three—dimensional tracking pattern of the human patella," *Journal of Orthopaedic Research*, vol. 8, no. 3, pp. 372–382, 1990.

[34] R. P. Welsh, "Knee joint structure and function," *Clinical Orthopaedics and Related Research*, vol. 147, pp. 7–14, 1980.

[35] Y.-F. Hsieh, L. F. Draganich, S. H. Ho, and B. Reider, "The effects of removal and reconstruction of the anterior cruciate ligament on patellofemoral kinematics," *The American Journal of Sports Medicine*, vol. 26, no. 2, pp. 201–209, 1998.

[36] H. Kurosawa, P. S. Walker, S. Abe, A. Garg, and T. Hunter, "Geometry and motion of the knee for implant and orthotic design," *Journal of Biomechanics*, vol. 18, no. 7, pp. 487–499, 1985.

[37] S. Nakagawa, Y. Kadoya, S. Todo et al., "Tibiofemoral movement 3: full flexion in the living knee studied by MRI," *Journal of Bone and Joint Surgery B*, vol. 82, no. 8, pp. 1199–1200, 2000.

[38] E. M. Abdel-Rahman and M. S. Hefzy, "Three-dimensional dynamic behaviour of the human knee joint under impact loading," *Medical Engineering and Physics*, vol. 20, no. 4, pp. 276–290, 1998.

[39] P. Wretenberg, D. K. Ramsey, and G. Németh, "Tibiofemoral contact points relative to flexion angle measured with MRI," *Clinical Biomechanics*, vol. 17, no. 6, pp. 477–485, 2002.

[40] P. A. Torzilli, R. Grigiene, J. Borrelli Jr., and D. L. Helfet, "Effect of impact load on articular cartilage: cell metabolism and viability, and matrix water content," *Journal of Biomechanical Engineering*, vol. 121, no. 5, pp. 433–441, 1999.

[41] P. F. Hill, V. Vedi, A. Williams, H. Iwaki, V. Pinskerova, and M. A. R. Freeman, "Tibiofemoral movement 2: the loaded and unloaded living knee studied by MRI," *Journal of Bone and Joint Surgery B*, vol. 82, no. 8, pp. 1196–1198, 2000.

[42] A. B. Zavatsky, P. T. Oppold, and A. J. Price, "Simultaneous in vitro measurement of patellofemoral kinematics and forces," *Journal of Biomechanical Engineering*, vol. 126, no. 3, pp. 351–356, 2004.

[43] T. M. G. J. Van Eijden, W. De Boer, and W. A. Weijs, "The orientation of the distal part of the quadriceps femoris muscle as a function of the knee flexion-extension angle," *Journal of Biomechanics*, vol. 18, no. 10, pp. 803–809, 1985.

[44] M. S. Hefzy, W. T. Jackson, S. R. Saddemi, and Y.-F. Hsieh, "Effects of tibial rotations on patellar tracking and patellofemoral contact areas," *Journal of Biomedical Engineering*, vol. 14, no. 4, pp. 329–343, 1992.

[45] R. Singerman, "Effects of patella alta and patella infera on patellofemoral contact forces," *Journal of Biomechanics*, vol. 27, no. 8, pp. 1059–1065, 1994.

[46] R. D. Komistek, D. A. Dennis, J. A. Mabe, and S. A. Walker, "An in vivo determination of patellofemoral contact positions," *Clinical Biomechanics*, vol. 15, no. 1, pp. 29–36, 2000.

[47] T. Suzuki, A. Hosseini, J.-S. Li, T. J. Gill, and G. Li, "In vivo patellar tracking and patellofemoral cartilage contacts during dynamic stair ascending," *Journal of Biomechanics*, vol. 45, no. 14, pp. 2432–2437, 2012.

[48] G. B. Salsich, S. R. Ward, M. R. Terk, and C. M. Powers, "In vivo assessment of patellofemoral joint contact area in individuals who are pain free," *Clinical Orthopaedics and Related Research*, no. 417, pp. 277–284, 2003.

[49] T. Farquhar, Y. Xia, K. Mann et al., "Swelling and fibronectin accumulation in articular cartilage explants after cyclical impact," *Journal of Orthopaedic Research*, vol. 14, no. 3, pp. 417–423, 1996.

[50] S. J. Mulholland and U. P. Wyss, "Activities of daily living in non-Western cultures: range of motion requirements for hip and knee joint implants," *International Journal of Rehabilitation Research*, vol. 24, no. 3, pp. 191–198, 2001.

Hindawi Publishing Corporation
The Scientific World Journal
Volume 2014, Article ID 785175, 7 pages
http://dx.doi.org/10.1155/2014/785175

Research Article

Squatting-Related Tibiofemoral Shear Reaction Forces and a Biomechanical Rationale for Femoral Component Loosening

Ashvin Thambyah[1] and Justin Fernandez[2,3]

[1] *Department of Chemical and Materials Engineering, University of Auckland, 20 Symonds Street, Auckland 1142, New Zealand*
[2] *Auckland Bioengineering Institute, University of Auckland, 70 Symonds Street, Auckland 1010, New Zealand*
[3] *Department of Engineering Science, University of Auckland, 70 Symonds Street, Auckland 1010, New Zealand*

Correspondence should be addressed to Ashvin Thambyah; ashvin.thambyah@auckland.ac.nz

Received 12 March 2014; Accepted 15 March 2014; Published 20 May 2014

Academic Editor: Shunji Hirokawa

Previous gait studies on squatting have described a rapid reversal in the direction of the tibiofemoral joint shear reaction force when going into a full weight-bearing deep knee flexion squat. The effects of such a shear reversal have not been considered with regard to the loading demand on knee implants in patients whose activities of daily living require frequent squatting. In this paper, *the shear reversal effect* is discussed and simulated in a finite element knee implant-bone model, to evaluate the possible biomechanical significance of this effect on femoral component loosening of high flexion implants as reported in the literature. The analysis shows that one of the effects of the shear reversal was a switch between large compressive and large tensile principal strains, from knee extension to flexion, respectively, in the region of the anterior flange of the femoral component. Together with the known material limits of cement and bone, this large mismatch in strains as a function of knee position provides new insight into how and why knee implants may fail in patients who perform frequent squatting.

1. Introduction

There is still much to be done to improve the design of knee implants both in terms of longevity and their ability to serve a wider range of patient needs. One particular need involves improving knee implant design to satisfy populations requiring a postoperative ability to perform deep knee bending and squatting [1–3]. The urgency of this problem is exacerbated by the increasing medical needs of aging Asian populations [4], in which deep knee bending and squatting are common activities of daily living, presenting the call for better design in implants that will allow deep flexion to be performed safely and reliably, without affecting the expected longevity of the implant.

High flexion knee replacement strategies have included retaining the cruciate ligament, specific intraoperative soft tissue balancing, and specially designed knee implants that control femoral rollback, improve joint conformity in large flexion angles, or provide more freedom in axial rotation [5]. Despite these efforts, studies have reported relatively limited long-term success [6–9], with femoral component loosening being identified as one of the more common negative outcomes in high-flexion knee arthroplasty. Such femoral component loosening, evident by radiolucency beneath the anterior flange [6], when investigated further revealed failure at the cement-metal interface. However rather than the technique or implant used, it has been suggested that the likely critical factor in determining the long-term outcome appears to be linked to the postoperative high-flexion activities [6, 10, 11], where in the femoral component "loosened" group the mean maximum postoperative knee flexion angle was significantly larger. Further it was found that loosened femoral components migrated towards a more flexed position [6].

That such femoral component migration from loosening of the femoral component, associated with cement-metal failure, which in turn is linked to postoperative weight-bearing high-flexion activities, indicates a strong biomechanical causative factor to the problem. Studies from

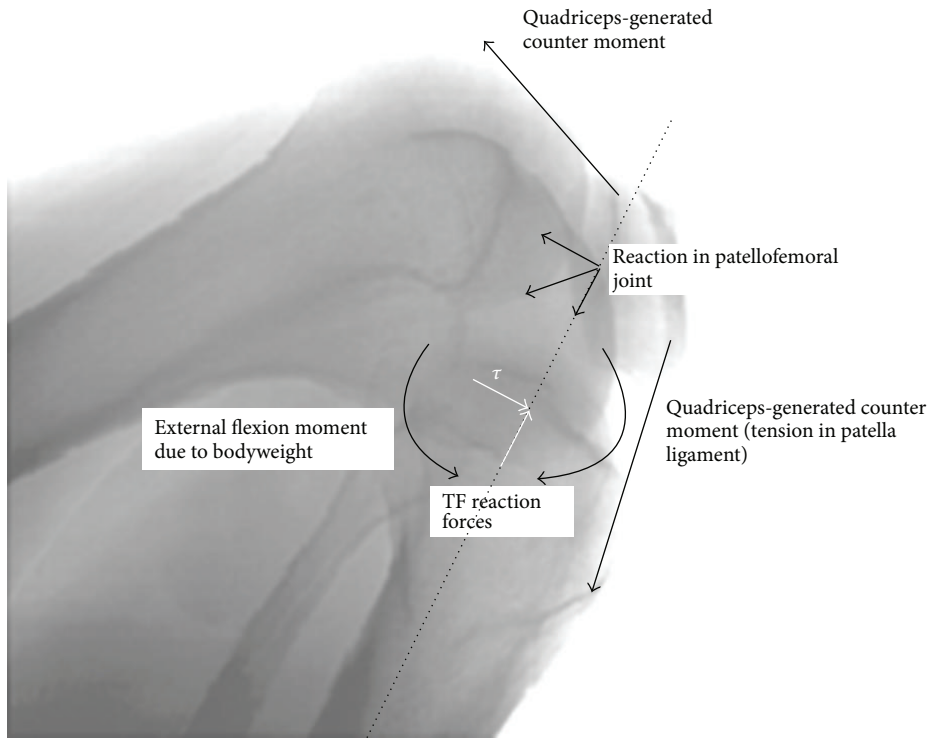

Figure 1: Schematic to illustrate how external flexion moments from reaction to body weight are balanced by internally generated moments from quadriceps activity. A backdrop of an X-ray image of a full squat is used as a reference. The reactions at the knee (illustrated as white arrows) show a compression and anterior-directed shear (τ).

a mechanical standpoint have shown that the possible causes for the loosening could be due to the altered kinematics and increased bicondylar rollback in deep flexion [13], absence of femoral load sharing with the bone [14], and being less than ideal strength in the cement-metal interface [15]. These three mechanical factors may not only be interrelated, but also be individualised targets for finding a solution to the loosening problem. However it is important to note that the primary cause is yet to be determined and there still is further insight to be gained from seeking out what could be the mechanism that initiates the failure in the system.

In this paper, we report on a hypothesis on what could be an important mechanical factor that initiates anterior flange femoral component loosening. This hypothesis is based on (i) earlier studies carried out on normal knee deep flexion and squatting kinematics and kinetics, (ii) a finite element method (FEM) analysis, and (iii) known properties and strength of the implant-cement-bone interfaces.

2. Materials and Methods

2.1. Knee Joint Kinematics and Kinetics in Squatting. From gait studies it was found that in Asian-style squatting the knee flexes up to 150° and the tibiofemoral contact forces are as high as 3 to 4 times body weight [12, 16]. Translating the contact forces into stresses, in vitro studies on human cadaver knees showed that the peak pressures can be as high as 20 MPa as a result of the drastic reduction in contact area [17]. Coupled with high stresses, the external rotation of the femur about the tibia ranged from 10° to over 20° and from 2 mm to 4 mm posterior translation of the femur [17, 18], and it was found that in Japanese knees the posterior translation was twice that of Caucasian knees [18]. The extent of this movement was attributed to the differing surface contact morphology of the medial versus lateral tibial plateaus [19]. Importantly, the posterior translation of the femur over the tibia during the squat would result in an anterior-directed shear reaction force in the tibiofemoral joint (Figure 1). This kinematic feature of squatting, the anterior-directed shear, has received little attention in the literature, given that in walking and standing the shear reaction force is largely posterior-directed and in going into a squat the shear reverses into an anterior-directed one [12] (Figure 2). It is this mechanism that informs our hypothesis for femoral component loosening in the high flexion knee implants and provides the loading condition for our model.

2.2. Finite Element Analysis Model. A finite element simulation was set up in Abaqus (Simulia) to evaluate the stress at the femoral bone-implant interface, specifically on the anterior flange. A generic knee model [20, 21] was developed and interfaced with a standard total knee replacement (TKR) configuration that consisted of cobalt chrome alloy femoral component, titanium tibial tray, polyethylene tibial insert, and polyethylene patellar button. The simulation was solved quasi-statically using Abaqus Standard with isotropic, linear

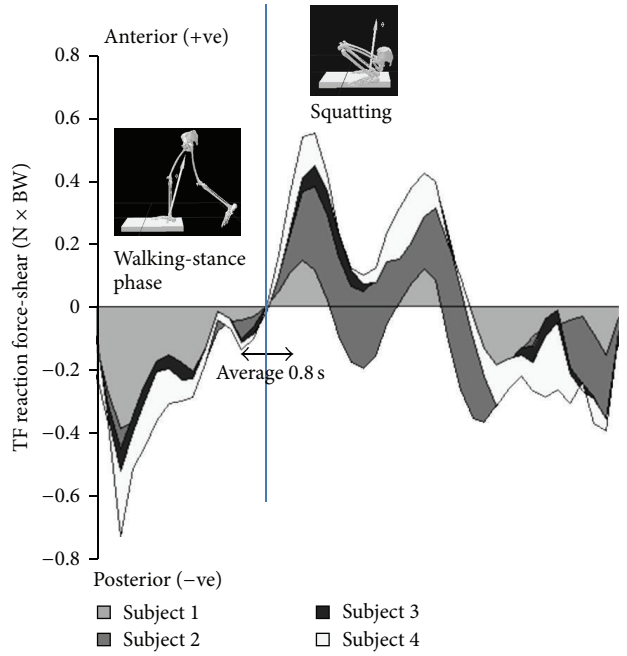

Figure 2: (Adapted from [12]), the reversal in shear reaction force in the tibiofemoral joint when the subject goes into a squat.

elastic material properties. The Young's modulus of titanium, cobalt chrome alloy, polyethylene, and the cortical bone was set to 110 GPa, 220 GPa, 686 Mpa, and 15 GPa, respectively [22, 23]. The bone cement was assumed to be a rigid bond. Ligament and patellar tendon material stiffness properties were taken as 300 Nmm^{-1} [23]. We examined the change in anterior flange stress and strain due solely to the change in the externally applied shear stress reaction direction. We simulated two poses, the knee in (a) relative extension during the single-limb weight bearing mid-stance phase of the gait cycle and (b) deep squatting at 150° of flexion. The tibia was fixed in both cases and a vertical compressive force of 1750 N (2.5 BW) and a horizontal shear force of 450 N (0.68 BW) were applied. These forces were to create the reaction forces at the tibiofemoral joint described in an earlier study [12] (see Figure 2). In knee extension an anterior shear force was applied to the femur to give rise to a posterior shear reaction force at the tibiofemoral joint. In knee flexion it was *reversed* to give rise to an anterior shear reaction force (Figure 3).

2.3. Known Properties and Strength of the Implant-Cement-Bone Interfaces. There are two interfaces, the implant-cement and the cement-bone. These interfaces have different strengths and can be directly attributed to the type of surface involved. For example, surface finish in metals [24–26] and bone preparation for cement to engage cortical versus cancellous bone [15] all have an influence on the final achievable mechanical strength of the bond. The static *shear* strength of the implant-cement interface ranges from 3 MPa to 16 MPa, depending on the surface finish of the metal implant [24]. Tensile strength is found to be lower than shear [27] ranging between 0.58 and 6.67 MPa. For the cement-bone interface, depending on bone surface roughness, the shear strength involving cancellous bone is 3.85 MPa and the tensile strength is much lower at 1.79 MPa [15]. This finding is consistent with an earlier study showing that the cement-bone interface is weaker in tension than in shear [28]. Bone cement properties are also reported in terms of microstrain.

3. Results

To compare the von Mises stresses between the knee extension and knee flexion positions, a sagittal section of the model was made and the strain distribution was plotted in terms of a colour map (Figure 4). The model revealed that stresses ranged from 5 MPa (dark blue) to a maximum of 20 MPa (red) with bone showing low stresses near the anterior flange for both knee extension and flexion (Figure 4). It appeared that stress was primarily borne by the femoral component except where the implant interfaces with the bone at the site of tibial contact at the knee extension position.

Of more interest were the principal strain values. To compare the maximum principal strains between the knee extension and knee flexion positions, a sagittal section of the model was made and the strain distribution was plotted in terms of a colour map (Figure 5). The strain ranged from a compressive normal strain of −2000 $\mu\varepsilon$ (dark blue) in the knee extension position to a *tensile* normal strain of +3000 $\mu\varepsilon$ (red) in full flexion. In knee extension the bulk of the bony strain was located near the inferior femoral condyles adjacent to the point of tibial contact. Also in this knee position, the maximum bone strain near the anterior flange occurred as two "hot-spots" (Figure 5(a), in blue within the dotted region) of compressive strain.

In contrast during deep knee flexion, and near the anterior flange, bone strain values were mostly tensile and spread over a much broader region along the length of the flange. The strain near the anterior flange during deep knee flexion exhibited a large mismatch between the bone and femoral component, where in the bone there is an overall larger region of high tensile strain compared to the femoral component (compare, e.g., regions of red in Figure 5(b)).

4. Discussion

For this study we only examined the influence of sagittal plane vertical and shear forces applied at the tibiofemoral contact, as the aim was to see the effect on the anterior flange region following a reversal of the shear direction. Any post-cam effects were not modeled and we argue that the transient anterior shear reaction that develops on going into a squat [12], meaning the femur tends to move posteriorly relative to the tibia, would not result in significant post-cam engagement. The effects of the femoral-patella contact or thigh-calf contact were also not modeled and it is without doubt that these would be important for any full knee flexion loading simulation [29]. However, these effects may not influence this study's focus on the anterior flange region for the following reasons. Firstly, in deep flexion, it is very likely that the femoral-patella contact, being very proximal

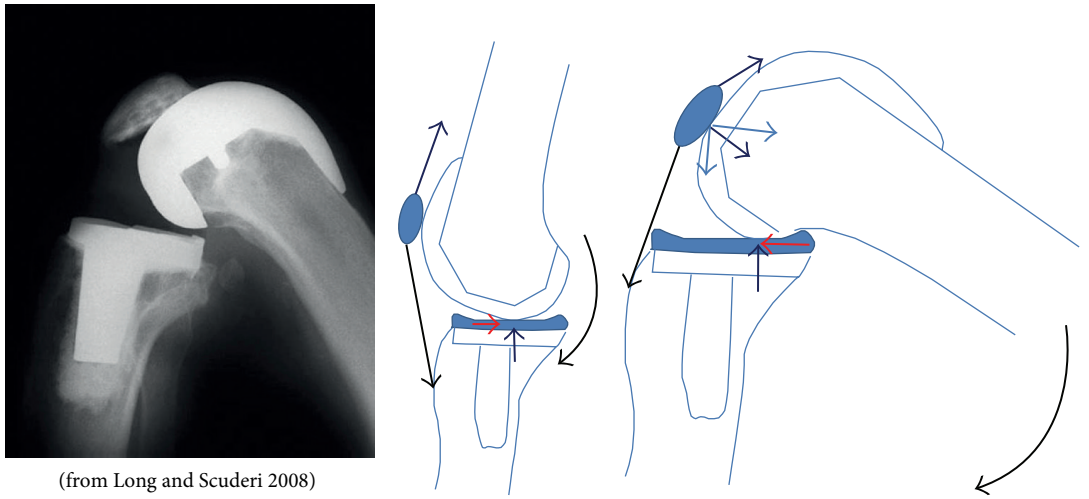

Figure 3: (a) Picture from [5], showing X-ray of implanted knee in deep flexion. (This picture has been rotated here to be consistent with the accompanying schematics.) (b) Force diagram to show the knee in extension. The short black and red arrows represent vertical and horizontal (shear) reactions in the tibiofemoral joint. The long arrows attached to the patella represent the force vectors of the patella tendon and ligament. The curved arrow represents the external moments acting on the knee, here in single-limb stance. (c) Force diagram showing the knee going into a squat. Note the reversal in shear (red arrow).

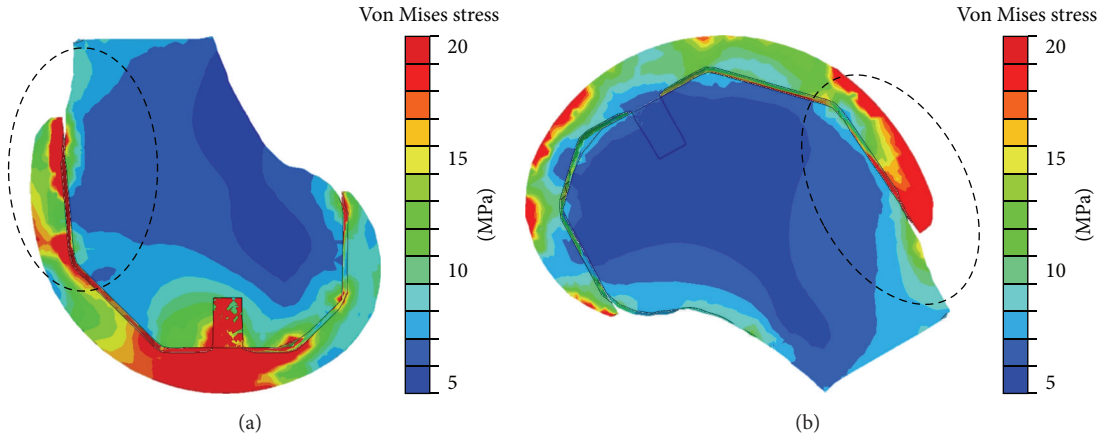

Figure 4: Sagittal cross-section of von Mises stress for (a) extended knee configuration and (b) deep knee flexion of 150°. Red is 20 MPa and dark blue is 5 MPa. The anterior flange region is circled.

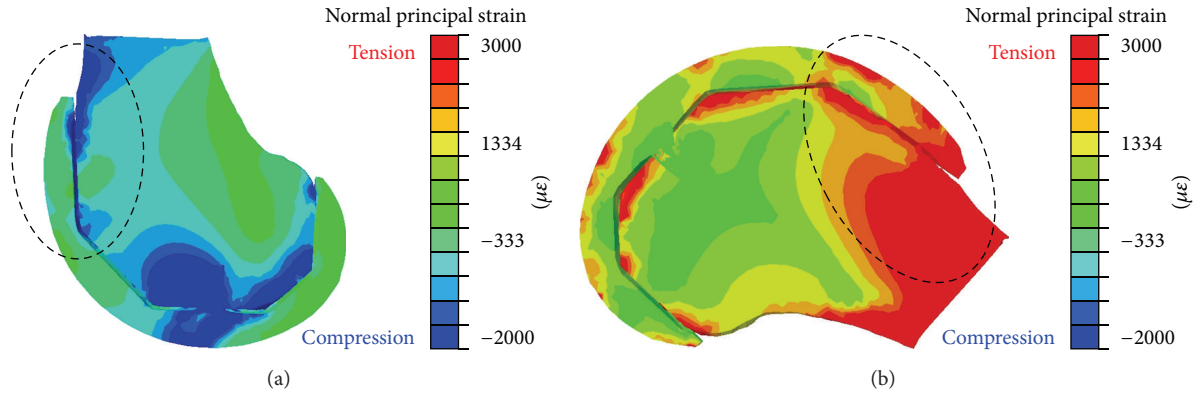

Figure 5: Sagittal cross-section of normal principal strains for (a) extended knee configuration and (b) deep knee flexion of 150°. Red is tension with a maximum of 3000 $\mu\varepsilon$ and dark blue is compression at −2000 $\mu\varepsilon$. The anterior flange region is circled.

to the joint line (Figure 3(a)), and from observation of the force diagram (Figure 3(c)), will result in moments that tend to bend the femur with respect to the femoral implant (Figure 6). Such bending stresses will thus tend to add to the bone bending stresses in the femur, confirmed by the increased tensile strain (shown in red in Figure 3(b)), in the distal femoral shaft in the knee flexion position. Secondly, the application of the shear reversal follows the gait data obtained previously [12] that was shown to happen prior to the rest phase in squat when the thigh contacts the calf. Hence, the simulation used in the present study, albeit simple in its approach, we argue, is valid for investigating a direct cause-effect relationship between the applied shear at the tibiofemoral joint and the resulting stresses and strain at the anterior flange.

The effects following the shear reversal, when the knee is in the flexed position, are larger von Mises stresses at the anterior flange region. The von Mises stresses provide a more realistic means of predicting failure criteria based on the combined effects of multidirectional stresses, as opposed to a unidirectional one. Therefore that the range of values for the ultimate stress for the implant-cement-bone interfaces, as described earlier in the methods section, is below the approximately 20 MPa high von Mises stress at the anterior flange region for the knee flexed position indicates that tibiofemoral shear reversal may be a causative factor for problems at this region in high flexion cases.

In addition, the tensile strains at the anterior flange for the knee flexed position, compared with the extension position where the strains in the same region were mostly compressive, provide additional insight into how the shear reversal effect may be detrimental to the implanted joint. In terms of maximum strains, the 3000 $\mu\varepsilon$ measured in the present model simulation of knee deep flexion is well below the failure range between 15,000 $\mu\varepsilon$ and 250,000 $\mu\varepsilon$ [30], meaning that the strain measured may not be of concern in terms of a single cycle static strain. However, taken into context of cyclic loading and creep, it would be a different matter. Previous experiments on bone cement strength have shown that 1000 $\mu\varepsilon$ results in failure after 10 million cycles [31]. The question then would be if such a lifespan could be reduced by (1) periodic interjections of 3000 $\mu\varepsilon$ tensile loading on going into and coming up from a squat, (2) possible sustained loading during the squatting phase [32] resulting in bone cement creep effects [33–35], and (3) bone cement being weakest in tension [15, 28, 36].

Furthermore, from the simulation (Figure 5) comparing extension to deep flexion, the high strain gradient from compression to tension, which when considering would be occurring rapidly [12] and bone cement as being a viscoelasticmaterial, may make the material increasingly strain limiting [37, 38] and susceptible to cracking. In addition the large mismatch in strain magnitude and strain pattern at the bone-implant anterior flange interface for deep flexion may lead to implant loosening due to failure of the bone cement in these regions. To note as well is the increased bone strain at levels of 3000 $\mu\varepsilon$ for deep knee flexion, in the distal femur near the anterior shaft all along to beneath the flange, which may lead to increased bone damage. Importantly, at these levels, damaged bone may be resorbed [39], which may then predispose the implant to loosening.

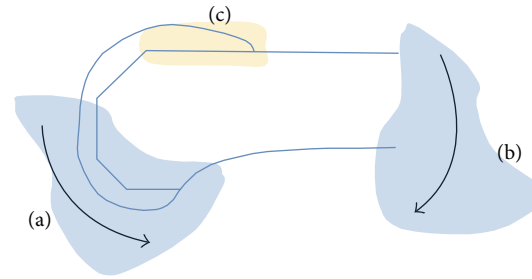

Figure 6: Schematic showing how the joint contact forces (vertical, shear, tibiofemoral, and patellofemoral) at (a) would be diametrically opposite the external body weight moment at (b) to create bending effects at (c).

5. Conclusions

To conclude, we deduce that the rapid reversal of the tibiofemoral shear reaction, from going into and coming up from a squat, constitutes a significant biomechanical factor for the possible failure mechanisms reported involving high flexion knee femoral component loosening. This rapid shear reversal, if incorporated into simulated loadings of implants in in vitro materials testing systems, may provide further insight into mechanisms of implant failure typically attributed to deep flexion knee activity.

Conflict of Interests

The authors declare that there is no conflict of interests regarding the publication of this paper.

References

[1] T. W. Kim, A. Makani, R. Choudhury, A. F. Kamath, and G. C. Lee, "Patient-reported activity levels after successful treatment of infected total knee arthroplasty," *The Journal of Arthroplasty*, no. 8, supplement, pp. 81–85, 2012.

[2] J. M. Weiss, P. C. Noble, M. A. Conditt et al., "What functional activities are important to patients with knee replacements?" *Clinical Orthopaedics and Related Research*, no. 404, pp. 172–188, 2002.

[3] K. K. Park, K. S. Shin, C. B. Chang, S. J. Kim, and T. K. Kim, "Functional disabilities and issues of concern in female Asian patients before TKA," *Clinical Orthopaedics and Related Research*, vol. 461, pp. 143–152, 2007.

[4] "WHO final report of the project, medical devices: managing the mismatch," the First WHO Global Forum on Medical Devices, 2010, http://www.who.int/medical_devices/access/en/.

[5] W. J. Long and G. R. Scuderi, "High-flexion total knee arthroplasty," *The Journal of Arthroplasty*, vol. 23, no. 7, supplement, pp. 6–10, 2008.

[6] H. S. Han, S.-B. Kang, and K. S. Yoon, "High incidence of loosening of the femoral component in legacy posterior stabilised-flex total knee replacement," *Journal of Bone and Joint Surgery B*, vol. 89, no. 11, pp. 1457–1461, 2007.

[7] W.-H. Jung, J.-H. Jeong, Y.-C. Ha, Y.-K. Lee, and K.-H. Koo, "High early failure rate of the Columbus posterior stabilized high-flexion knee prosthesis," *Clinical Orthopaedics and Related Research*, vol. 470, no. 5, pp. 1472–1481, 2012.

[8] J. Zelle, D. Janssen, J. van Eijden, M. de Waal Malefijt, and N. Verdonschot, "Does high-flexion total knee arthroplasty promote early loosening of the femoral component?" *Journal of Orthopaedic Research*, vol. 29, no. 7, pp. 976–983, 2011.

[9] E. K. Song, S. J. Park, T. R. Yoon, K. S. Park, H. Y. Seo, and J. K. Seon, "Hi-flexion and gender-specific designs fail to provide significant increases in range of motion during cruciate-retaining total knee arthroplasty," *The Journal of Arthroplasty*, vol. 27, no. 6, pp. 1081–1084, 2012.

[10] C. W. Han, I. H. Yang, W. S. Lee, K. K. Park, and C. D. Han, "Evaluation of postoperative range of motion and functional outcomes after cruciate-retaining and posterior-stabilized high-flexion total knee arthroplasty," *Yonsei Medical Journal*, vol. 53, no. 4, pp. 794–800, 2012.

[11] S.-D. Cho, Y.-S. Youm, and K.-B. Park, "Three- to six-year follow-up results after high-flexion total knee arthroplasty: can we allow passive deep knee bending?" *Knee Surgery, Sports Traumatology, Arthroscopy*, vol. 19, no. 6, pp. 899–903, 2011.

[12] A. Thambyah, "How critical are the tibiofemoral joint reaction forces during frequent squatting in Asian populations?" *The Knee*, vol. 15, no. 4, pp. 286–294, 2008.

[13] M. Tamaki, T. Tomita, T. Watanabe, T. Yamazaki, H. Yoshikawa, and K. Sugamoto, "In vivo kinematic analysis of a high-flexion, posterior-stabilized, mobile-bearing knee prosthesis in deep knee bending motion," *The Journal of Arthroplasty*, vol. 24, no. 6, pp. 972–978, 2009.

[14] P. Bollars, J.-P. Luyckx, B. Innocenti, L. Labey, J. Victor, and J. Bellemans, "Femoral component loosening in high-flexion total knee replacement: an in vitro comparison of high-flexion versus conventional designs," *Journal of Bone and Joint Surgery B*, vol. 93, no. 10, pp. 1355–1361, 2011.

[15] S. A. van de Groes, M. C. de Waal Malefijt, and N. Verdonschot, "Influence of preparation techniques to the strength of the bone-cement interface behind the flange in total knee arthroplasty," *The Knee*, vol. 20, no. 3, pp. 186–190, 2013.

[16] T. Nagura, H. Matsumoto, Y. Kiriyama, A. Chaudhari, and T. P. Andriacchi, "Tibiofemoral joint contact force in deep knee flexion and its consideration in knee osteoarthritis and joint replacement," *Journal of Applied Biomechanics*, vol. 22, no. 4, pp. 305–313, 2006.

[17] A. Thambyah, J. C. H. Goh, and S. Das De, "Contact stresses in the knee joint in deep flexion," *Medical Engineering and Physics*, vol. 27, no. 4, pp. 329–335, 2005.

[18] S. Nakagawa, Y. Kadoya, S. Todo et al., "Tibiofemoral movement 3: full flexion in the living knee studied by MRI," *Journal of Bone and Joint Surgery B*, vol. 82, no. 8, pp. 1199–1200, 2000.

[19] M. A. R. Freeman and V. Pinskerova, "The movement of the knee studied by magnetic resonance imaging," *Clinical Orthopaedics and Related Research*, no. 410, pp. 35–43, 2003.

[20] J. W. Fernandez, P. Mithraratne, S. F. Thrupp, M. H. Tawhai, and P. J. Hunter, "Anatomically based geometric modelling of the musculo-skeletal system and other organs," *Biomechanics and Modeling in Mechanobiology*, vol. 2, no. 3, pp. 139–155, 2004.

[21] J. W. Fernandez and P. J. Hunter, "An anatomically based patient-specific finite element model of patella articulation: towards a diagnostic tool," *Biomechanics and Modeling in Mechanobiology*, vol. 4, no. 1, pp. 20–38, 2005.

[22] H. J. Kim, J. W. Fernandez, M. Akbarshahi, J. P. Walter, B. J. Fregly, and M. G. Pandy, "Evaluation of predicted knee-joint muscle forces during gait using an instrumented knee implant," *Journal of Orthopaedic Research*, vol. 27, no. 10, pp. 1326–1331, 2009.

[23] P. Beillas, G. Papaioannou, S. Tashman, and K. H. Yang, "A new method to investigate in vivo knee behavior using a finite element model of the lower limb," *Journal of Biomechanics*, vol. 37, no. 7, pp. 1019–1030, 2004.

[24] H. Zhang, L. T. Brown, L. A. Blunt, and S. M. Barrans, "Influence of femoral stem surface finish on the apparent static shear strength at the stem-cement interface," *Journal of the Mechanical Behavior of Biomedical Materials*, vol. 1, no. 1, pp. 96–104, 2008.

[25] B. Beksac, N. A. Taveras, A. G. D. Valle, and E. A. Salvati, "Surface finish mechanics explain different clinical survivorship of cemented femoral stems for total hip arthroplasty," *Journal of Long-Term Effects of Medical Implants*, vol. 16, no. 6, pp. 407–422, 2006.

[26] K. L. Ohashi, A. C. Romero, P. D. McGowan, W. J. Maloney, and R. H. Dauskardt, "Adhesion and reliability of interfaces in cemented total joint arthroplasties," *Journal of Orthopaedic Research*, vol. 16, no. 6, pp. 705–714, 1998.

[27] J. Zelle, D. Janssen, S. Peeters, C. Brouwer, and N. Verdonschot, "Mixed-mode failure strength of implant-cement interface specimens with varying surface roughness," *Journal of Biomechanics*, vol. 44, no. 4, pp. 780–783, 2011.

[28] K. A. Mann, F. W. Werner, and D. C. Ayers, "Mechanical strength of the cement-bone interface is greater in shear than in tension," *Journal of Biomechanics*, vol. 32, no. 11, pp. 1251–1254, 1999.

[29] S. van de Groes, M. de Waal-Malefijt, and N. Verdonschot, "Probability of mechanical loosening of the femoral component in high flexion total knee arthroplasty can be reduced by rather simple surgical techniques," *The Knee*, vol. 21, no. 1, pp. 209–215, 2014.

[30] J. P. Davies, D. O. O'Connor, J. A. Greer, and W. H. Harris, "Comparison of the mechanical properties of Simplex P, Zimmer Regular, and LVC bone cements," *Journal of Biomedical Materials Research*, vol. 21, no. 6, pp. 719–730, 1987.

[31] J. P. Davies, D. W. Burke, D. O. O'Connor, and W. H. Harris, "Comparison of the fatigue characteristics of centrifuged and uncentrifuged Simplex P bone cement," *Journal of Orthopaedic Research*, vol. 5, no. 3, pp. 366–371, 1987.

[32] Y. Zhang, D. J. Hunter, M. C. Nevitt et al., "Association of squatting with increased prevalence of radiographic tibiofemoral knee osteoarthritis: the Beijing osteoarthritis study," *Arthritis and Rheumatism*, vol. 50, no. 4, pp. 1187–1192, 2004.

[33] O. Kuzmychov, C. Koplin, R. Jaeger, H. Büchner, and U. Gopp, "Physical aging and the creep behavior of acrylic bone cements," *Journal of Biomedical Materials Research B: Applied Biomaterials*, vol. 91, no. 2, pp. 910–917, 2009.

[34] D. G. Kim, M. A. Miller, and K. A. Mann, "Creep dominates tensile fatigue damage of the cement-bone interface," *Journal of Orthopaedic Research*, vol. 22, no. 3, pp. 633–640, 2004.

[35] T. L. Norman, V. Kish, J. D. Blaha, T. A. Gruen, and K. Hustosky, "Creep characteristics of hand- and vacuum-mixed acrylic bone cement at elevated stress levels," *Journal of Biomedical Materials Research*, vol. 29, no. 4, pp. 495–501, 1995.

[36] E. I. Gates, D. R. Carter, and W. H. Harris, "Tensile fatigue failure of acrylic bone cement," *Journal of Biomechanical Engineering*, vol. 105, no. 4, pp. 393–397, 1983.

[37] G. Lewis, "Viscoelastic properties of injectable bone cements for orthopaedic applications: state-of-the-art review," *Journal of Biomedical Materials Research Part B: Applied Biomaterials*, vol. 98, no. 1, pp. 171–191, 2011.

[38] G. Lewis, "Properties of acrylic bone cement: state of the art review," *Journal of Biomedical Materials Research*, vol. 38, no. 2, pp. 155–182, 1997.

[39] H. M. Frost, "Wolff's Law and bone's structural adaptations to mechanical usage: an overview for clinicians," *Angle Orthodontist*, vol. 64, no. 3, pp. 175–188, 1994.

Hindawi Publishing Corporation
The Scientific World Journal
Volume 2014, Article ID 695028, 7 pages
http://dx.doi.org/10.1155/2014/695028

Research Article

The Effect of Malrotation of Tibial Component of Total Knee Arthroplasty on Tibial Insert during High Flexion Using a Finite Element Analysis

Kei Osano,[1] Ryuji Nagamine,[1] Mitsugu Todo,[2] and Makoto Kawasaki[3]

[1] *Sugioka Memorial Hospital, Bone and Joint Center, 3-6-1 Kashiiteriha, Higashi-ku, Fukuoka 813-0017, Japan*
[2] *Research Institute for Applied Mechanics, Kyushu University, 6-1 Kasuga-koen, Kasuga, Fukuoka 816-8580, Japan*
[3] *School of Medicine, University of Occupational and Environmental Health, 1-1 Iseigaoka, Yahata-nishi-ku, Kitakyushu, Fukuoka 807-8555, Japan*

Correspondence should be addressed to Kei Osano; k_osano@sugioka-mh.jp

Received 28 February 2014; Accepted 25 March 2014; Published 8 May 2014

Academic Editors: F. Berto and B. F. Yousif

One of the most common errors of total knee arthroplasty procedure is a malrotation of tibial component. The stress on tibial insert is closely related to polyethylene failure. The objective of this study is to analyze the effect of malrotation of tibial component for the stress on tibial insert during high flexion using a finite element analysis. We used Stryker NRG PS for analysis. Three different initial conditions of tibial component including normal, 15° internal malrotation, and 15° external malrotation were analyzed. The tibial insert made from ultra-high-molecular-weight polyethylene was assumed to be elastic-plastic while femoral and tibial metal components were assumed to be rigid. Four nonlinear springs attached to tibial component represented soft tissues around the knee. Vertical load was applied to femoral component which rotated from 0° to 135° while horizontal load along the anterior posterior axis was applied to tibial component during flexion. Maximum equivalent stresses on the surface were analyzed. Internal malrotation caused the highest stress which arose up to 160% of normal position. External malrotation also caused higher stress. Implanting prosthesis in correct position is important for reducing the risk of abnormal wear and failure.

1. Introduction

Total knee arthroplasty (TKA) has been a common surgical treatment for severe osteoarthritis of the knee. High knee flexion after TKA is of increasing concern for people who are younger and more physically active as well as people living in the Middle East and Asia where high flexion is culturally required for activities of daily living [1]. Advancement of TKA prostheses design contributed to the improvement of clinical performance including a widened range of motion and a prolonged prosthesis survivorship. However, surgical procedure as well as prosthesis design is very important for knee kinematics and long-term survivorship of prosthesis. One of the most common procedure errors is a malrotation of tibial component [2]. Although the ideal axial alignment of tibial component is still being discussed [3–6], it was reported that malrotation affects the distribution of the stress on contact surface of tibial insert [7, 8], which might cause the early failure of tibial insert [9], and, moreover, leads to knee pain after TKA [2].

In the literature, several studies analyzed the stress on polyethylene insert and contact areas using computational models [9–19]. Although some of them used finite element analysis (FEA) [10–14, 16–18], most of their analyses focused on walking gait or static analysis [10, 14, 15]. A few studies used dynamic models to analyze the stress distribution [12, 16–18]. Our group developed simplified three-dimensional FEA models to reproduce the implanted knee kinematics and investigated the stress distribution on the tibial insert [16, 17]. The objective of this study is, therefore, to analyze the effect of malrotation of tibial component on tibial insert during squatting maneuver using our FEA model.

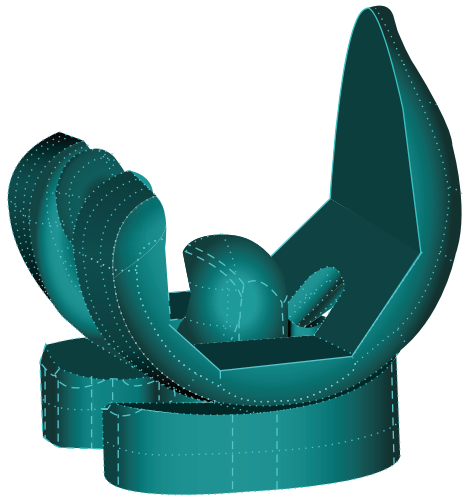

Figure 1: Prosthesis used in the current analysis. Femoral and tibial components are assumed to be rigid and UHMWPE tibial insert was assumed to be elastic-plastic. Two pegs of femoral component were removed for simplification.

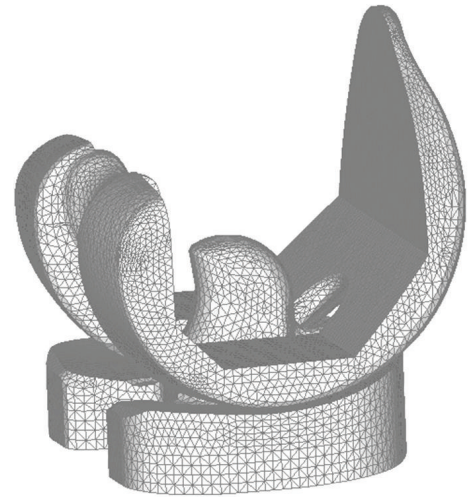

Figure 2: Mesh model of PS-type knee prosthesis for FEA analysis.

Table 1: Material constants of UHMWPE tibial insert.

Density (kg/m^3)	E (MPa)	ν (—)	σY (MPa)
940	800	0.4	16

2. Methods

A posterior-stabilized total knee prosthesis, Scorpio NRG (Stryker Co., Kalamazoo, USA) was used for analysis (Figure 1). The feature of tibial insert design is symmetrical and flat, which enables flexible axial rotation. Three-dimensional FEA models, consisting of femoral component, tibial insert, and tibial component, were constructed from the CAD data obtained from the manufacturer, as illustrated in Figure 2. Tetrahedral meshes were generated on these models by FEMAP ver. 9.2 (Siemens PLM Software, Plano, USA). The number of nodes and elements was 28,254 and 121,536, respectively. The tibial insert made from ultra-high-molecular-weight polyethylene (UHMWPE) was assumed to be elastic-plastic material and to follow von Mises yield criterion. The nonlinear stress-strain relationship experimentally obtained was used (Table 1, Figure 3) [20].

Femoral and tibial components made of Co-Cr alloy were assumed to be rigid for reducing computational complexity. A coefficient of friction of articular surface was set to be 0.04. Four nonlinear springs were attached to tibial component in order to represent soft tissues around the knee. Its nonlinear force-displacement relation was given by [14]

$$F = 0.18667d^2 + 1.3313d, \quad (1)$$

where F and d are force and displacement under a knee with cruciate ligaments removed.

Boundary conditions are shown in Figure 4. The femoral component was allowed to translate in the vertical direction and rotate about a transverse axis to simulate flexion and extension. The tibial component was allowed to translate in

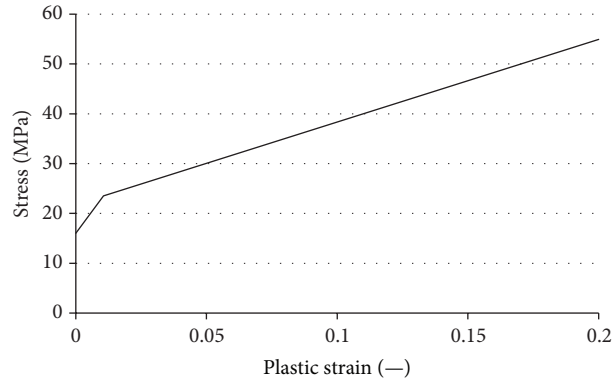

Figure 3: Bilinear relationship of stress-plastic strain curve of UHMWPE.

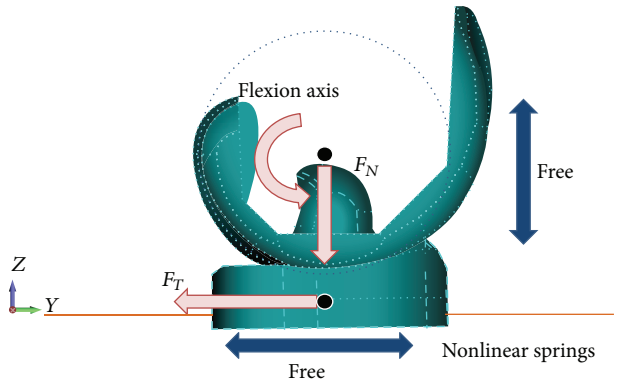

Figure 4: Boundary conditions of the current analysis. Femoral component is free along the vertical axis and rotates along the flexion axis. Tibial component is free along the AP axis and rotates along the vertical axis located at the center of component. The force F_N is applied to the femoral component and F_T is applied to the tibial component. Four linear springs, two in the front and two in the back, are attached to the tibial component in order to represent soft tissues around the knee.

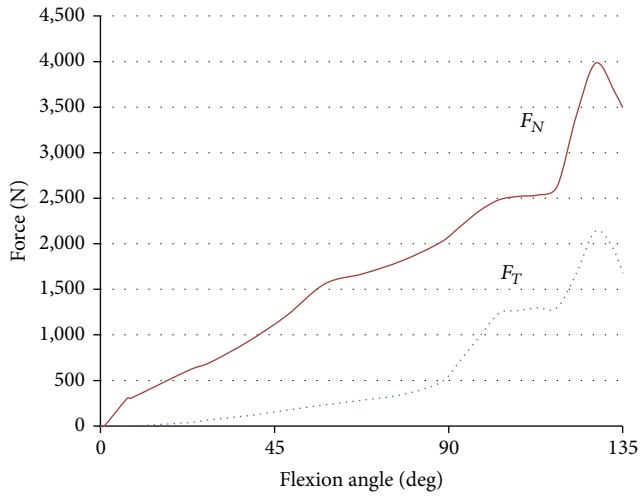

Figure 5: Force-flexion angle relationship of loading conditions. F_N is vertical load applied to the femoral component and F_T is horizontal load applied to the tibial component.

the AP direction and rotate about a vertical axis located in the center of tibial condyles to simulate internal and external rotation [15]. Load conditions were referred to in the previous analysis [21]. Vertical load was applied to the femoral component which rotated from 0° to 135° of flexion while horizontal load along the AP direction was applied to the tibial component which internally rotated from 0° to 15° of rotation during knee flexion. The amount of vertical load increased gradually to its maximum level of 4000 N around 130° of flexion and the amount of AP direction load increased to 2100 N at the same angle (Figure 5). Three different initial conditions of tibial components, normal (NRM), internally rotated for 15° (IR), and externally rotated for 15° (ER), were analyzed. In the current analysis, the rotational alignment of femoral component was defined as a line through the center of both femoral fixation pegs. The rotational alignment of the tibial component was defined as a line along the posterior border. Two lines were configured as parallel in NRM position.

For FEA, explicit finite element codes LS-DYNA ver. 971 and LS-PREPOST ver. 4.0 (Livermore Software Technology Co., Livermore, USA) were utilized as a solver and a postprocessor. The maximum von Mises stress on post surface and condyle surface of tibial insert was analyzed separately.

3. Results

Figures 6, 7, and 8 show contours of maximum von Mises equivalent stress on tibial insert of NRM, IR, and ER positions at the flexion angle of 45°, 90°, and 135°. Concentrated stress on the edge of tibial insert was observed at 135° in NRM position and at 90° and 135° in IR malposition. ER malposition had no elevation of stress level on the edge.

The history of maximum Mises equivalent stress on the insert is shown in Figure 9. In each rotational position, the stress on post surface rapidly increased after the post-cam engagement which occurred at around 60° of knee flexion. Although ER malposition led almost to the same pattern of stress history as NRM position, IR malposition caused significant increase in the stress on post surface under high flexion (Figure 9(a)). The level of the stress of post surface in IR at 120° of flexion was 1.6 times as that in NRM. The stress on condyle surface was also high in IR malposition throughout knee flexion. ER malposition increased the stress on condyle surface under midflexion compared to NRM position (Figure 9(b)).

4. Discussion

Rotational alignment of femoral and tibial components affects the stress distribution on contact surface. Wear and fracture of polyethylene is a common complication of TKA. Biomechanical studies have demonstrated that the stress in polyethylene component is closely related to polyethylene failure [13]. There are many patterns in polyethylene damage, including crack, wear, and delamination [22, 23]. Sirimamilla et al. showed that peak stress caused crack propagation in cross-linked UHMWPE [24]. Accumulated crack could lead to delamination in the subsurface region. As the number of TKA performed is increasing and the procedure is performed on more culturally diverse populations, high flexion of the knee is in high demand. The result of the current study implies that malrotation of the tibial component increases the risk of early failure of the tibial polyethylene insert [14] and the impingement of components which could affect range of motion and lead to stiff knees [25]. Some of the revision surgeries are related to these complications. It is, therefore, important to analyze the effect of malposition on tibial inserts. Many researchers have investigated polyethylene wear using various analytical methods such as FEA and experimental measurement. Most studies, however, assumed normal position of each component [11]. A few studies, to our knowledge, have analyzed the effect of malrotation of tibial component using FEA.

Matsuda et al. investigated the contact stress on various types of tibial insert under 15° of malrotation of tibial component [8]. They used an electronic sensor to detect contact location in cadaver knees; then they measured peak and mean stresses on the insert under compressive load. Their results showed that the contact stresses were higher when tibial component was implanted in malrotation position. The stress levels were more than double compared to those of the neutral position. Our result was consistent with Matsuda's study.

Liau et al. investigated the effects of malalignment on stresses on tibial insert of total knee prostheses by calculating the contact stress and von Mises stress using FEA [13]. They constructed three different prostheses designs, the high conformity flat-on-flat design, high conformity curve-on-curve design, and medium conformity curve-on-curve design at a neutral alignment and three different malalignment models including the medial translation, internal rotation, and varus tilt of femoral component relative to the tibial component.

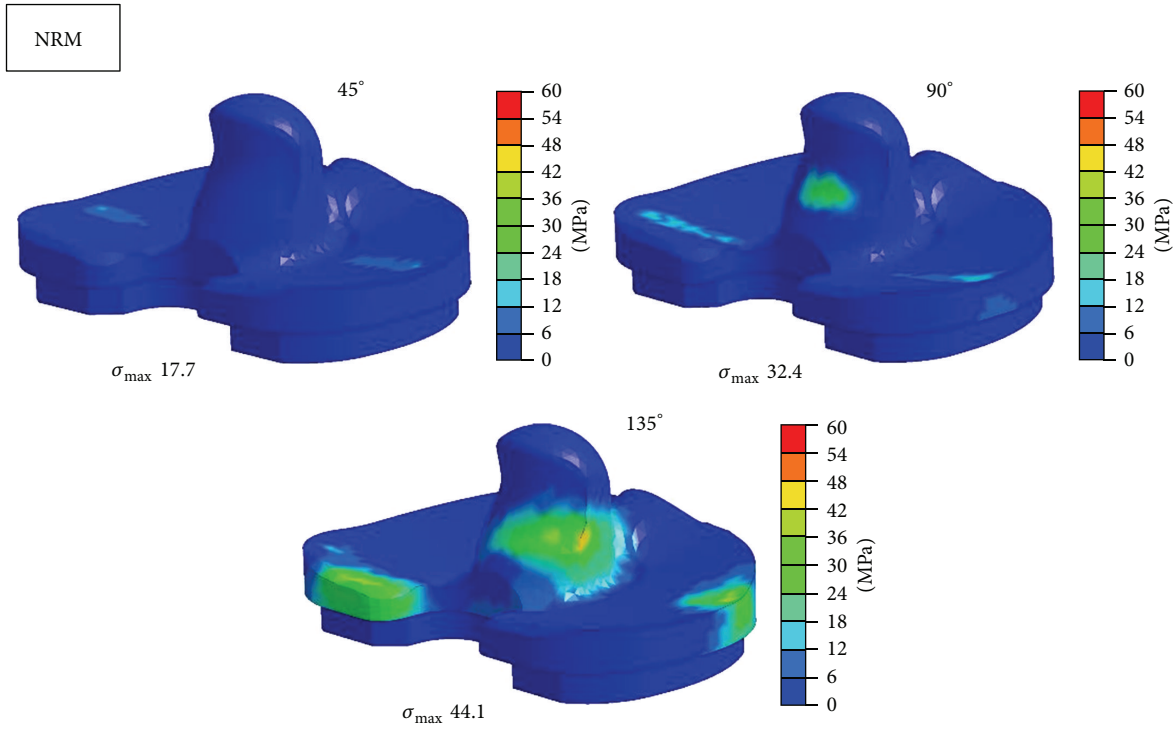

Figure 6: Maximum equivalent stress distribution in tibial insert at each position at the flexion angle of 45°, 90°, and 135°. σ_{max} = maximum equivalent stress. NRM = normal.

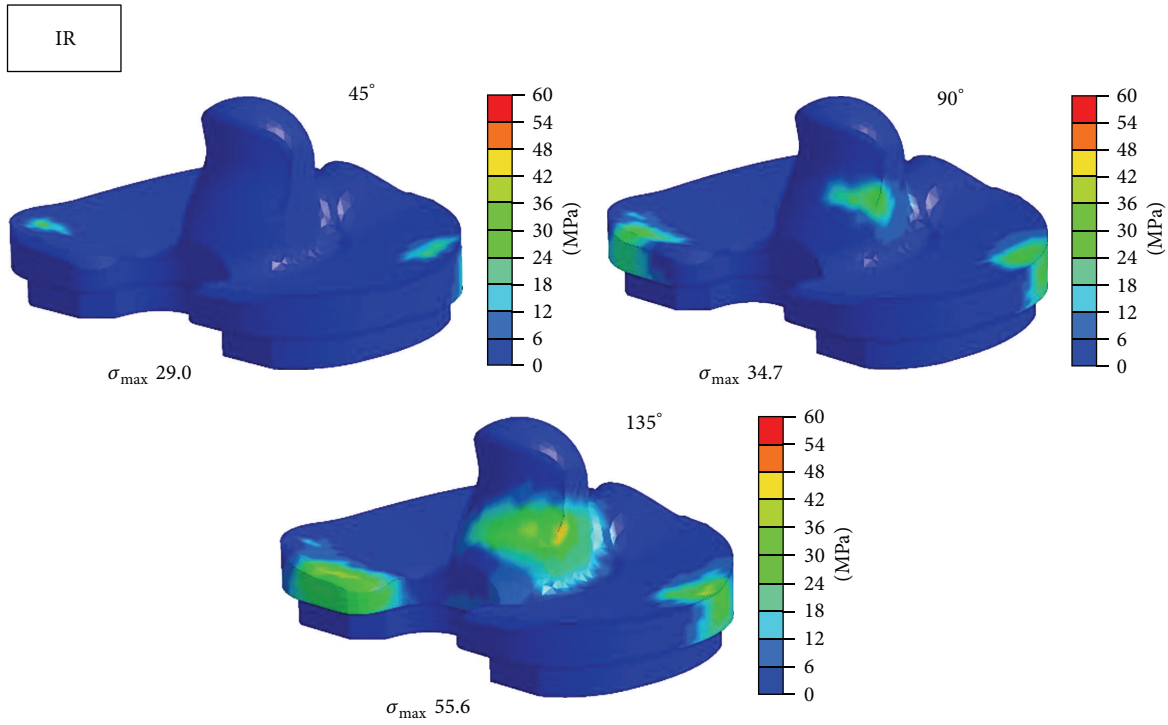

Figure 7: Maximum equivalent stress distribution in tibial insert at each position at the flexion angle of 45°, 90°, and 135°. σ_{max} = maximum equivalent stress. IR = internal rotation.

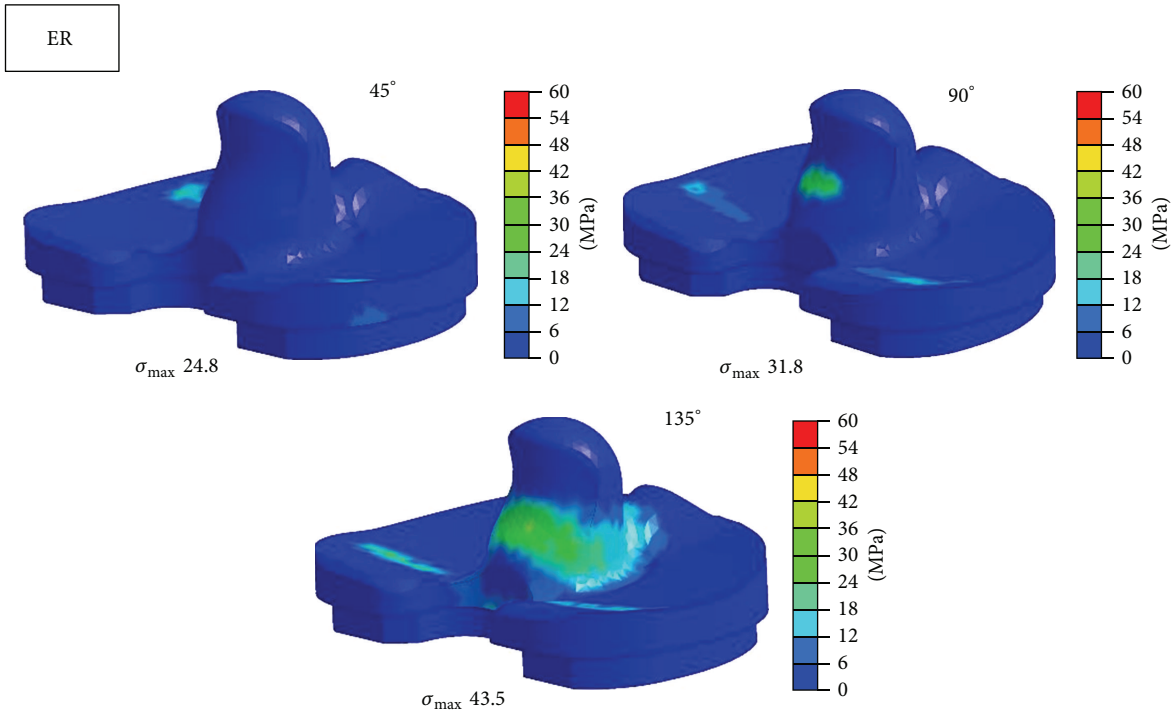

Figure 8: Maximum equivalent stress distribution in tibial insert at each position at the flexion angle of 45°, 90°, and 135°. σ_{max} = maximum equivalent stress. ER = external rotation.

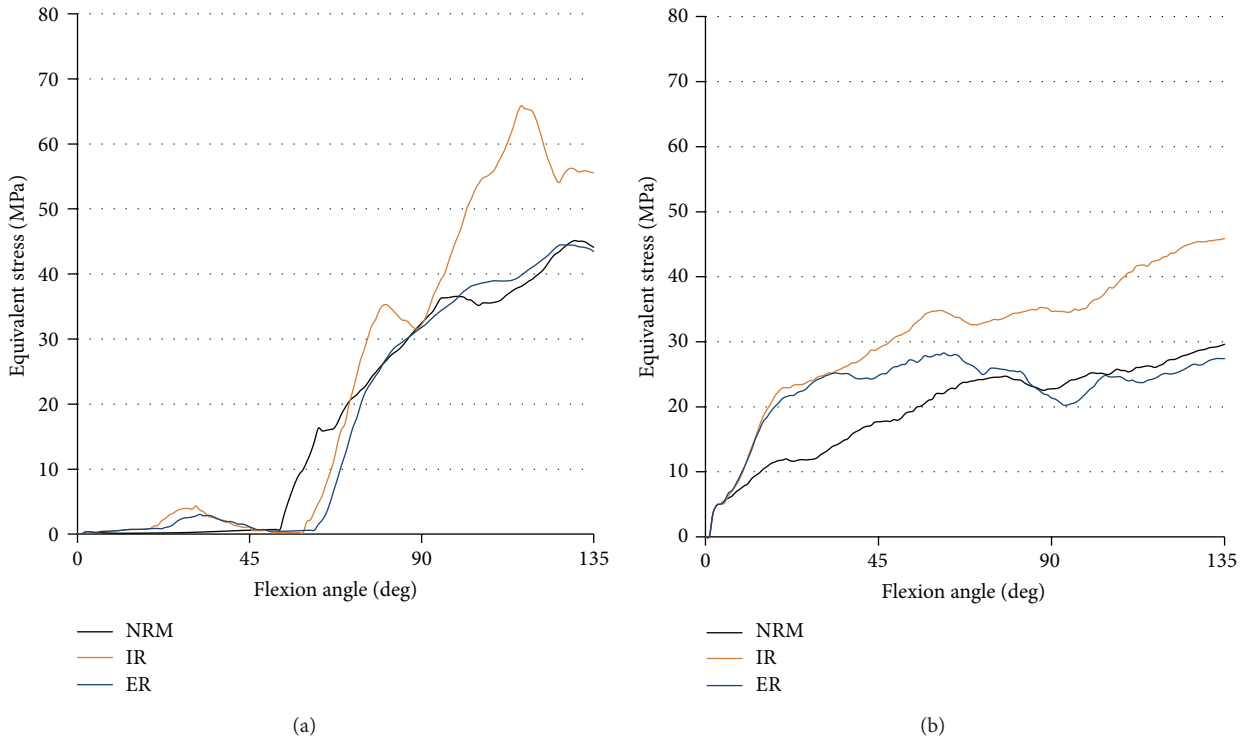

Figure 9: The equivalent stress (MPa) on tibial insert at each flexion angle. (a) Stress on post surface. (b) Stress on condyle surface.

Compression load was applied to the tibiofemoral joint at extended knee position. Their results showed that each malalignment model had higher stress on tibial insert and malrotation led relatively to lower stress on tibial insert than other malalignments. The maximum von Mises stress increased about 15% in internal malrotation. However, their analysis, like other studies using FEA, was under static condition. Our results revealed that internal rotation malrotation of tibial component for 15° increased the stress on tibial insert by more than 50% during high flexion of the knee.

Innocenti et al. investigated the sensitivity of patellofemoral and tibiofemoral contact forces to patient-related anatomical factors and component position in the different TKA prosthesis types including two types of fixed bearing prosthesis and two types of mobile bearing prosthesis [12]. Each prosthesis was virtually implanted on the cadaver leg model and it underwent a loaded squat between 0° and 120°. Their results showed that tibiofemoral contact forces are mostly affected by an anatomical location of medial collateral ligament. Their results showed that malrotation of tibial components also played a role in increasing tibiofemoral contact force by up to 16% in fixed bearing TKA models. The reason why this percentage is much lower than our result is that they set 5° of malrotation in their analysis. Moreover, different prosthesis design would have different pattern of stress distribution and stress level.

There are several limitations in the current study. First, every FEA has boundary conditions. Squatting is produced by muscle force and regulated by many soft tissues. In the current analysis, we applied vertical load to the femoral component and horizontal load on the tibial component and attached four springs to the tibial component so as to represent soft tissues around the knee joint. Although it is difficult to reproduce in vivo kinematics of the knee on computer simulation, parameters in the current study had been all experimentally examined and our model demonstrated the roll-back motion of the knee. Moreover, the stress level of our analysis was assumed to be consistent with previous study. Akasaki et al. investigated the contact stress on post surface using the same prosthesis as our analysis and the stress level at 90° of knee flexion was 35 MPa which was almost the same as our result [7]. Therefore, we consider our results as valid. Secondly, we did not consider the cyclic loading. We analyzed the stress on tibial insert during single squatting. Polyethylene wear was generated as a result of repeated loading on the surface. Finally, we analyzed one prosthesis which has relatively flat tibiofemoral joint. When we extend the current analysis to other prostheses such as more high conformity design prosthesis, the results would be different. Further investigation would be expected for future studies.

As the tibial insert of NRG is symmetrical and flat, the prosthesis is recognized to have a considerable extent of flexibility for axial malrotation. However, the results of this study revealed that excessive internal rotation malrotation increased the stress on tibial insert significantly. Therefore, internal rotation malrotation should be avoided when we use this prosthesis.

5. Conclusion

Although Stryker NRG has a flat design which produces flexible axial rotation, according to the current study, internal malrotation of tibial component caused a significant increase of stress level on tibial polyethylene insert. To reduce the risk of early failure of tibial insert, it is important to avoid internal malrotation of tibial component.

Conflict of Interests

The authors declare that there is no conflict of interests regarding the publication of this paper.

Acknowledgment

The authors would like to thank Mr. Mohd Afzan Mohd Anuar for technical and editorial support.

References

[1] E. A. Morra and A. S. Greenwald, "Polymer insert stress in total knee designs during high-flexion activities: a finite element study," *The Journal of Bone & Joint Surgery A*, vol. 87, no. 12, pp. 120–124, 2005.

[2] D. Nicoll and D. Rowley, "Tibial component malrotation is a major cause of pain after total knee replacement," *The Journal of Bone & Joint Surgery*, vol. 91, supplement 1, pp. 30–31, 2009.

[3] M. Akagi, M. Oh, T. Nonaka, H. Tsujimoto, T. Asano, and C. Hamanishi, "An anteroposterior axis of the tibia for total knee arthroplasty," *Clinical Orthopaedics and Related Research*, vol. 420, no. 3, pp. 213–219, 2004.

[4] J. P. Cobb, H. Dixon, W. Dandachli, and F. Iranpour, "The anatomical tibial axis: reliable rotational orientation in knee replacement," *The Journal of Bone & Joint Surgery B*, vol. 90, no. 8, pp. 1032–1038, 2008.

[5] M. Ikeuchi, N. Yamanaka, Y. Okanoue, E. Ueta, and T. Tani, "Determining the rotational alignment of the tibial component at total knee replacement," *The Journal of Bone & Joint Surgery B*, vol. 89, no. 1, pp. 45–49, 2007.

[6] R. Rossi, M. Bruzzone, D. E. Bonasia, A. Marmotti, and F. Castoldi, "Evaluation of tibial rotational alignment in total knee arthroplasty: a cadaver study," *Knee Surgery, Sports Traumatology, Arthroscopy*, vol. 18, no. 7, pp. 889–893, 2010.

[7] Y. Akasaki, S. Matsuda, T. Shimoto, H. Miura, H. Higaki, and Y. Iwamoto, "Contact stress analysis of the conforming post-cam mechanism in posterior-stabilized total knee arthroplasty," *The Journal of Arthroplasty*, vol. 23, no. 5, pp. 736–743, 2008.

[8] S. Matsuda, S. E. White, V. G. Williams II, D. S. McCarthy, and L. A. Whiteside, "Contact stress analysis in meniscal bearing total knee arthroplasty," *The Journal of Arthroplasty*, vol. 13, no. 6, pp. 699–706, 1998.

[9] S. P. Ahir, G. W. Blunn, H. Haider, and P. S. Walker, "Evaluation of a testing method for the fatigue performance of total knee tibial trays," *Journal of Biomechanics*, vol. 32, no. 10, pp. 1049–1057, 1999.

[10] A. C. Godest, M. Beaugonin, E. Haug, M. Taylor, and P. J. Gregson, "Simulation of a knee joint replacement during a gait cycle using explicit finite element analysis," *Journal of Biomechanics*, vol. 35, no. 2, pp. 267–275, 2002.

[11] J. P. Halloran, A. J. Petrella, and P. J. Rullkoetter, "Explicit finite element modeling of total knee replacement mechanics," *Journal of Biomechanics*, vol. 38, no. 2, pp. 323–331, 2005.

[12] B. Innocenti, S. Pianigiani, L. Labey, J. Victor, and J. Bellemans, "Contact forces in several TKA designs during squatting: a numerical sensitivity analysis," *Journal of Biomechanics*, vol. 44, no. 8, pp. 1573–1581, 2011.

[13] J.-J. Liau, C.-K. Cheng, C.-H. Huang, and W.-H. Lo, "The effect of malalignment on stresses in polyethylene component of total knee prostheses—a finite element analysis," *Clinical Biomechanics*, vol. 17, no. 2, pp. 140–146, 2002.

[14] S. Sathasivam and P. S. Walker, "A computer model with surface friction for the prediction of total knee kinematics," *Journal of Biomechanics*, vol. 30, no. 2, pp. 177–184, 1997.

[15] M. Taylor and D. S. Barrett, "Explicit finite element simulation of eccentric loading in total knee replacement," *Clinical Orthopaedics and Related Research*, vol. 414, pp. 162–171, 2003.

[16] J. A. Thompson, M. W. Hast, J. F. Granger, S. J. Piazza, and R. A. Siston, "Biomechanical effects of total knee arthroplasty component malrotation: a computational simulation," *Journal of Orthopaedic Research*, vol. 29, no. 7, pp. 969–975, 2011.

[17] M. Todo, R. Nagamine, and S. Yamaguchi, "Stress analysis of PS type knee prostheses under deep flexion," *Journal of Biomechanical Science and Engineering*, vol. 2, no. 4, pp. 237–245, 2007.

[18] M. Todo, Y. Takahashi, and R. Nagamine, "Stress analysis of artificial knee joints under flexion and rotation," *Tribology Online*, vol. 3, no. 3, pp. 211–215, 2008.

[19] R. von Eisenhart-Rothe, T. Vogl, K.-H. Englmeier, and H. Graichen, "A new in vivo technique for determination of femoro-tibial and femoro-patellar 3D kinematics in total knee arthroplasty," *Journal of Biomechanics*, vol. 40, no. 14, pp. 3079–3088, 2007.

[20] K. Kobayashi, T. Kakinoki, Y. Tanabe, and M. Sakamoto, "Mechanical properties of ultra-high molecular weight polyethylene under impact compression—property change with gamma irradiation and dynamic stress-strain analysis of artificial hip joint," *Journal of the Japanese Society For Experimental Mechanics*, vol. 3, pp. 225–229, 2005.

[21] N. J. Dahlkvist, P. Mayo, and B. B. Seedhom, "Forces during squatting and rising from a deep squat," *Engineering in Medicine*, vol. 11, no. 2, pp. 69–76, 1982.

[22] M. K. Harman, J. Desjardins, L. Benson, S. A. Banks, M. Laberge, and W. A. Hodge, "Comparison of polyethylene tibial insert damage from in vivo Function and in vitro wear simulation," *Journal of Orthopaedic Research*, vol. 27, no. 4, pp. 540–548, 2009.

[23] M. S. Kuster and G. W. Stachowiak, "Factors affecting polyethylene wear in total knee arthroplasty," *Orthopedics*, vol. 25, supplement 2, pp. s235–s242, 2002.

[24] A. Sirimamilla, J. Furmanski, and C. Rimnac, "Peak stress intensity factor governs crack propagation velocity in crosslinked ultrahigh-molecular-weight polyethylene," *Journal of Biomedical Material Research B: Applied Biomaterials*, vol. 101, no. 3, pp. 430–435, 2013.

[25] M. Bédard, K. G. Vince, J. Redfern, and S. R. Collen, "Internal rotation of the tibial component is frequent in stiff total knee arthroplasty," *Clinical Orthopaedics and Related Research*, vol. 469, no. 8, pp. 2346–2355, 2011.

Hindawi Publishing Corporation
The Scientific World Journal
Volume 2014, Article ID 205375, 6 pages
http://dx.doi.org/10.1155/2014/205375

Review Article

Biomechanical Considerations in the Design of High-Flexion Total Knee Replacements

Cheng-Kung Cheng,[1,2] Colin J. McClean,[1] Yu-Shu Lai,[2] Wen-Chuan Chen,[2] Chang-Hung Huang,[3] Kun-Jhih Lin,[4] and Chia-Ming Chang[1]

[1] *Institute of Biomedical Engineering, National Yang-Ming University, No. 155, Section 2, Linong Street, Beitou District, Taipei 11221, Taiwan*
[2] *Orthopaedic Device Research Center, National Yang-Ming University, No. 155, Section 2, Linong Street, Beitou District, Taipei 11221, Taiwan*
[3] *Department of Medical Research, Mackay Memorial Hospital, New Taipei City 10499, Taiwan*
[4] *Center of Translation Technology for Medical Device, Chung Yuan Christian University, Taoyuan 32023, Taiwan*

Correspondence should be addressed to Cheng-Kung Cheng; ckcheng@ym.edu.tw and Yu-Shu Lai; yslai@ym.edu.tw

Received 28 February 2014; Accepted 25 March 2014; Published 6 May 2014

Academic Editors: S. Hirokawa, B. Mody, A. Thambyah, and M. Todo

Typically, joint arthroplasty is performed to relieve pain and improve functionality in a diseased or damaged joint. Total knee arthroplasty (TKA) involves replacing the entire knee joint, both femoral and tibial surfaces, with anatomically shaped artificial components in the hope of regaining normal joint function and permitting a full range of knee flexion. In spite of the design of the prosthesis itself, the degree of flexion attainable following TKA depends on a variety of factors, such as the joint's preoperative condition/flexion, muscle strength, and surgical technique. High-flexion knee prostheses have been developed to accommodate movements that require greater flexion than typically achievable with conventional TKA; such high flexion is especially prevalent in Asian cultures. Recently, computational techniques have been widely used for evaluating the functionality of knee prostheses and for improving biomechanical performance. To offer a better understanding of the development and evaluation techniques currently available, this paper aims to review some of the latest trends in the simulation of high-flexion knee prostheses.

1. Introduction

Many daily activities require considerable knee flexion, level walking >60°, ascending stairs >80°, sitting >90°, and getting out of a bath >130° [1, 2]. High-flexion often refers to movements that require over 120° of knee flexion, which are particularly common in Asian cultures [3–6], squatting, sitting cross-legged, kneeling, and prayer. High-flexion (HF) knee prostheses have been developed for this purpose and have been proven to accommodate such movements. However, whether such HF prostheses are clinically more effective than conventional knee replacements is debatable, with most studies showing either no significant improvement or mild improvements over conventional TKA [7–10]. Even for studies that do report significantly greater flexion with HF designs, bias in patient selection, experimental errors, or shortcomings in measurement methods may greatly influence the results [3–5]. Therefore, whether HF knee prostheses are practically useful to patients requires further research using clearly defined measurement and testing methods to make studies comparable.

The choice to use a high-flexion knee is ultimately left to the surgeon, with patient consent. As such, this report will compile published data regarding the biomechanical aspects of HF total knee replacement (TKR) with special focus on posterior cruciate ligament retaining knees (cruciate-retaining (CR)) and posterior cruciate ligament sacrificing designs (posterior-stabilized (PS)). Meta-analyses comparing CR and PS knees have generally shown no favourable design in terms of longevity, range of motion, and pain. A recent Cochrane Database review [11] of 17 studies involving 1810 patients concluded that there is no solid clinical reason for

choosing to either retain or remove the posterior cruciate ligament (PCL) but also noted that arthroplasty where the PCL is retained is more difficult to perform.

2. Modelling High Knee Flexion

This review details two computational methods for studying the biomechanics of knee prostheses. One method uses multibody dynamics software, namely, MSC Adams (MSC Software Corporation, Santa Ana, CA), to study the dynamic behaviour of the knee joint. Another technique is to use finite element analysis (FEA) to study the internal mechanical condition of the joint: stress, strain, and so forth. The FEA research detailed below typically used ABAQUS (Dassault Systèmes, Vélizy-Villacoublay, France) accompanied by some preprocessing and meshing software.

The major drawback in the computational simulation of joints lies in the simplifications that must be made within each model. Some of these assumptions are purposely designed into the model in consideration of cost, computing power, time, processing, and so forth, but it must also be noted that such simulations have not advanced far enough to realistically imitate all of the components and tissues within the joint. Inherent simplifications in the modelling process, such as inaccurate representations of soft tissues, need to be taken into consideration. The validity of a model may be determined by comparing the results against in/ex vivo studies of a representative human joint or by comparing the models against previously validated simulations. Each of the models detailed below has been validated in this manner.

3. Achieving High Knee Flexion

High knee flexion (>120°) requires significant translation of the femoral condyles on the tibial plateau. Inadequate femoral rollback and tibial rotation are common complications with current high-flexion prostheses during such high flexion [12–14]. To overcome these problems, Liu et al. developed a nonsymmetric CR tibial insert with a lateral condyle that was lowered and convex in shape, reportedly replicating the shape of a healthy knee [15, 16]. The convex insert allows the femoral condyle to sublux off the back of the tibial plateau and reduces the incidence of impingement during high flexion. Direct impingement between the posterior tibial insert and femur has been suggested as a factor limiting high flexion in conventional prostheses [17]. The concave radius of the medial condyle was also reduced to offer a tighter tibiofemoral contact. It was found that shaping the condyles of the CR TKR in this way increased femoral rollback and tibial internal rotation over a traditional symmetric TKR. However, it should be noted that beyond 100° knee flexion both the symmetric and nonsymmetric TKR models were reversed into external tibial rotation, but the intact (healthy) knee model continued to show internal rotation of the tibia [15]. So, while shaping the tibial insert similar to an intact knee does noticeably improve knee kinematics, it still cannot claim to accurately replicate the motion patterns of a healthy knee. A follow-up study modified the shape of both the medial and lateral condyles of the CR femoral component and included the aforementioned convex lateral tibial compartment (Figure 1) [18]. Rollback and rotation were compared to a symmetric TKR model. It was found that, by increasing the height of the medial femoral condyle over the lateral condyle, the model could demonstrate more natural knee motion from extension through to deep flexion, although this follow-up study did not directly compare the models against an intact knee. A general conclusion can be drawn that, by mimicking the convex shape of the lateral tibial insert and increasing the height of the medial femoral condyle over the lateral side, femoral rollback and tibial rotation can be improved.

Retrieval studies have consistently shown incongruent articular surfaces to be associated with a greater risk of polyethylene wear [19–21]. Increasing the conformity between the femoral and tibial surfaces and closely replicating the shape of the anatomical knee should help in reducing such wear. However, thinning the lateral compartment puts the insert at risk of fracture, and heightening the medial compartment may disrupt the joint line. Lin et al. [22] demonstrated that a 10 mm elevation of the joint line in a PS knee, by increasing the thickness of the tibial insert, significantly tensioned the collateral ligaments and increased joint stiffness. While stiffer ligaments may offer a more stable joint, such excessive stiffness as seen in Lin et al.'s study would place the joint under greater internal loading and possibly fracture the tibial insert. Further research is needed on this point to determine the optimal thickness of the insert and height difference between the medial and lateral compartments so as to offer the greatest biomechanical advantage without increasing the risk of component wear.

Additionally, mobile bearing tibial inserts have been developed to offer dual articulation in the knee, theoretically permitting a greater range of motion and reducing contact stress, and in turn reducing wear [19, 23]. In a series of case studies on retrieved implants, Huang et al. found such mobile bearings to produce smaller particulate debris and a higher percentage of granular debris in comparison to their fixed bearing counterparts, placing the knee at greater risk of osteolysis [24–26], but it was also noted that mobile bearing designs allow for earlier recognition of component wear [27].

It has been reported that at least 19% of patients receiving posterior stabilized (PS) knees suffer abnormal tibiofemoral axial rotation [7]. While the degree of tibial rotation is highly variable between different TKA studies, it is generally conceded that axial rotation following TKA cannot accurately replicate healthy knee motion. Li et al. [14] demonstrated the importance of the cam-spine (post-cam) mechanism in guiding tibiofemoral motion and that knee motion after engagement between the post and cam was quite independent of the applied muscle loads. However, in PS knees, the interaction between the cam and spine as the knee is flexed, particularly at high flexion angles, will heavily influence both the motion of the knee and the longevity of the implant itself; a greater contact area will increase stability and reduce localized contact stress on the spine. Lin et al. evaluated two different post-cam contact shapes in PS knees, with flat-on-flat or curve-on-curve surfaces (Figure 2) [28]. Tibial rotation

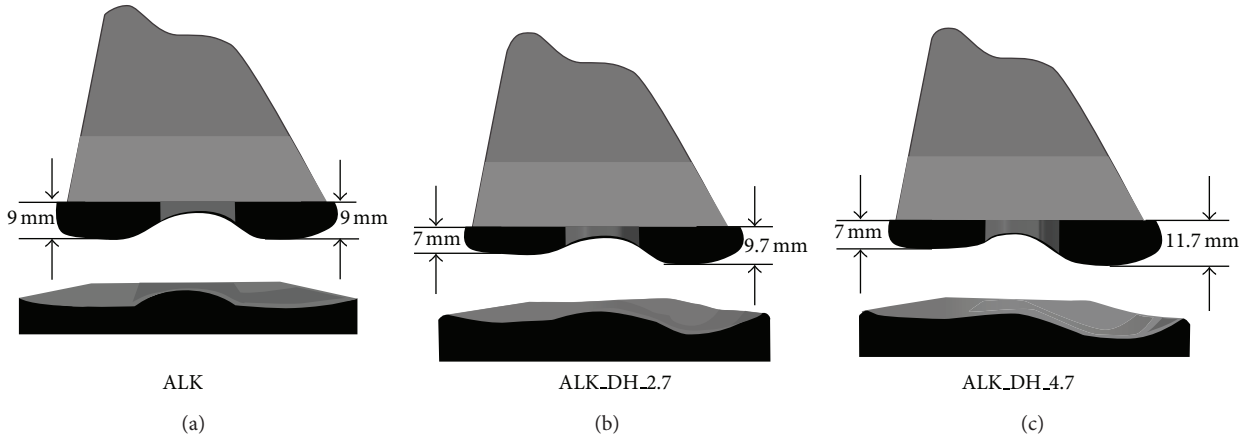

Figure 1: Femoral and tibial components modified on both medial and lateral sides [18]. (a) Anatomic-like knee, (b) knee with condyle height difference of 2.7 mm, and (c) knee with condyle height difference of 4.7 mm.

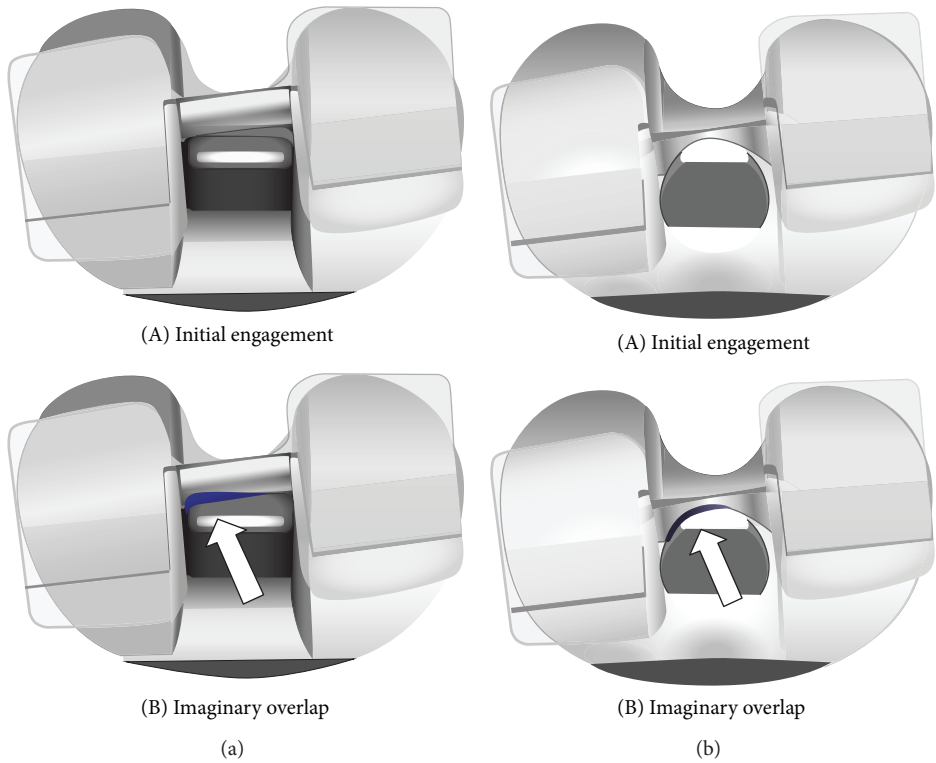

Figure 2: Initial engagement and the imaginary overlap between the tibial post and femoral cam for flat-on-flat (a) and curve-on-curve (b) models [28].

was shown to be comparable in both designs prior to post-cam engagement; an obvious deviation in plots was evident at around 45° knee flexion. The curve-on-curve design showed greater rotation beyond this point up to full flexion at 135°, although both designs followed a similar motion pattern. Figure 2 shows the overlap between the post and cam for both models during knee flexion. The greater medial impingement is obvious in the flat-on-flat model, which would increase edge loading on the post and also add resistance to tibial rotation.

In a related study, Huang et al. analysed the stress on the tibial post for flat-on-flat and curve-on-curve designs up to a knee flexion angle of 150° [29]. Two conditions were simulated, one where there was no rotation between the tibia and femur and the other with 10° internal rotation of the tibial insert relative to the femoral component, which is more representative of anatomical alignment. Wear of the tibial post is inevitable as the cam and spine engage and rub against each other during knee flexion, and this can often lead to fracture of the post. As in Lin et al.'s study [28], a flat-on-flat

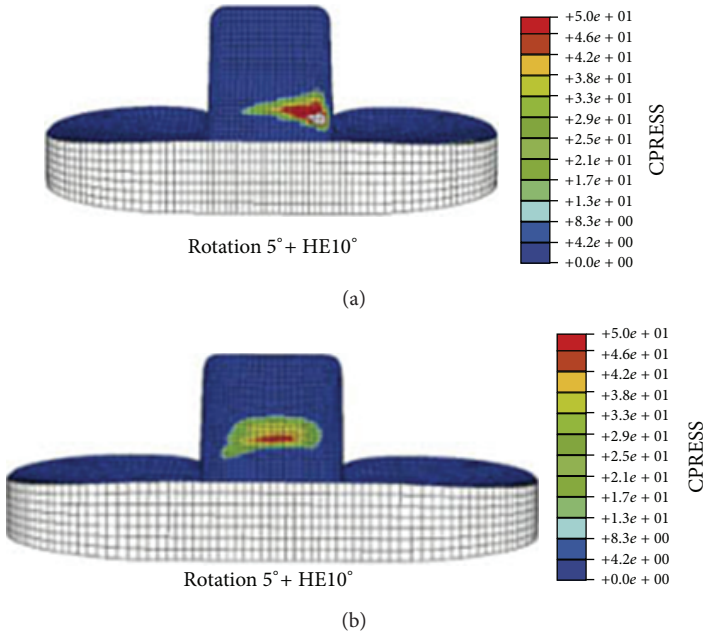

Figure 3: Contact stress (MPa) on the anterior face of tibial post at 10° hyperextension and 5° axial rotation for (a) flat-on-flat and (b) curve-on-curve contact surfaces (modified from [30]).

design can be expected to experience greater edge loading on the posterior face of the post as the tibia rotates out of neutral alignment with the femur. For the 10° rotation models, Huang et al. showed that curve-on-curve contact surfaces can reduce the maximum contact stress on the posterior tibial post by over 30% in comparison to flat-on-flat surfaces and can increase the contact area by 8%. In a follow-up study, Huang et al. examined the contact status on the anterior face of the tibial post where contact with the femoral component occurs when the knee is extended [30]. Knee prostheses were modelled with 0°, 2.5°, and 5° of axial rotation and in 0°, 5°, and 10° of hyperextension; intuitively, hyperextension of the knee may further increase the stress on the anterior post. By tilting the femoral component forward by 5°, putting it into hyperextension, and tilting the tibial insert posteriorly by 5°, Wang et al. were able to improve femoral rollback in comparison to a knee with components inserted in a neutral alignment [31]. However, while the medial condyle showed comparable motion to a healthy knee up to 135° knee flexion, rollback of the lateral condyle was greatly reduced. Correspondingly, Huang et al. [30] showed that 10° of hyperextenion (with 5° axial rotation) could reduce anterior curve-on-curve peak contact stress by 25% in comparison to flat-on-flat surfaces and could increase the contact area by about 30% (Figure 3). Figure 3 details the location of the maximum contact stress when the knee was hyperextended by 10°; significant edge loading is obvious in the flat-on-flat model. Huang et al. also observed that the contact point shifted downward as the degree of hyperextension was increased from 0° to 5° to 10° and noted that the shorter moment arm could reduce the tensile stress on the post. Putting the knee into hyperextension may lower the contact point on the tibial post and improve femoral rollback, which is important for high flexion, but it also increases the stress on the anterior face of the post in comparison to a knee in neutral alignment.

In a bid to further improve tibial rotation, Lin et al. [32] modified a curve-on-curve surface to reduce the thickness of the medial side of the curved femoral cam; the cam gradually reduced in thickness from the lateral to medial side. In comparison to a baseline curve-on-curve model, the asymmetric cam design was shown to improve tibial rotation, but medial femoral rollback was compromised. Even after post-cam engagement, the medial condyle of the femur was located anteriorly, which could lead to early impingement.

4. Conclusion

In conclusion, these studies promote the use of anatomically shaped knee prostheses to achieve high knee flexion while limiting component wear. A rounded and convex lateral plateau and a shallower medial plateau on the tibial surface promote femoral rollback and permit more natural knee motion. Also, the post-cam contact surfaces should be rounded on both the anterior and posterior faces to reduce edge loading and produce a greater contact surface area throughout flexion. As mentioned, an asymmetric curve-on-curve cam shape may improve tibial rotation but at the expense of femoral rollback.

Conflict of Interests

The authors declare that there is no conflict of interests regarding the publication of this paper.

Authors' Contribution

Cheng-Kung Cheng and Colin J. McClean contributed equally to this work.

References

[1] P. J. Rowe, C. M. Myles, C. Walker, and R. Nutton, "Knee joint kinematics in gait and other functional activities measured using flexible electrogoniometry: how much knee motion is sufficient for normal daily life?" *Gait & Posture*, vol. 12, no. 2, pp. 143–155, 2000.

[2] D. S. Jevsevar, P. O. Riley, W. A. Hodge, D. E. Krebs, and M. M. Rodgers, "Knee kinematics and kinetics during locomotor activities of daily living in subjects with knee arthroplasty and in healthy control subjects," *Physical Therapy*, vol. 73, no. 4, pp. 229–242, 1993.

[3] S. M. Acker, R. A. Cockburn, J. Krevolin, R. M. Li, S. Tarabichi, and U. P. Wyss, "Knee kinematics of high-flexion activities of daily living performed by Male Muslims in the Middle East," *The Journal of Arthroplasty*, vol. 26, no. 2, pp. 319–327, 2011.

[4] S. Tarabichi, Y. Tarabichi, A. R. Tarabishy, and M. Hawari, "Importance of full flexion after total knee replacement in Muslims' daily lifestyle," *Journal of the Islamic Medical Association of North America*, vol. 38, no. 1, pp. 17–22, 2006.

[5] S. J. Mulholland and U. P. Wyss, "Activities of daily living in non-Western cultures: range of motion requirements for hip and knee joint implants," *International Journal of Rehabilitation Research*, vol. 24, no. 3, pp. 191–198, 2001.

[6] M. S. Hefzy, B. P. Kelly, and T. D. V. Cooke, "Kinematics of the knee joint in deep flexion: a radiographic assessment," *Medical Engineering and Physics*, vol. 20, no. 4, pp. 302–307, 1998.

[7] D. Dennis, R. D. Heekin, C. R. Clark, J. A. Murphy, T. L. O'Dell, and K. A. Dwyer, "Effect of implant design on knee flexion," *The Journal of Arthroplasty*, vol. 28, no. 3, pp. 429–438, 2013.

[8] Y. S. Anouchi, M. McShane, F. Kelly Jr., J. Elting, and J. Stiehl, "Range of motion in total knee replacement," *Clinical Orthopaedics and Related Research*, no. 331, pp. 87–92, 1996.

[9] Y.-H. Kim, K.-S. Sohn, and J.-S. Kim, "Range of motion of standard and high-flexion posterior stabilized total knee prostheses: a prospective, randomized study," *The Journal of Bone & Joint Surgery A*, vol. 87, no. 7, pp. 1470–1475, 2005.

[10] R. W. Nutton, M. L. van der Linden, P. J. Rowe, P. Gaston, and F. A. Wade, "A prospective randomised double-blind study of functional outcome and range of flexion following total knee replacement with the NexGen standard and high flexion components," *The Journal of Bone & Joint Surgery B*, vol. 90, no. 1, pp. 37–42, 2008.

[11] W. C. Verra, L. G. van den Boom, W. Jacobs, D. J. Clement, A. A. Wymenga, and R. G. Nelissen, "Retention versus sacrifice of the posterior cruciate ligament in total knee arthroplasty for treating osteoarthritis," *Cochrane Database of Systematic Reviews*, no. 10, p. CD004803, 2013.

[12] T. P. Andriacchi and J. O. Galante, "Retention of the posterior cruciate in total knee arthroplasty," *The Journal of Arthroplasty*, vol. 3, pp. s13–s19, 1988.

[13] M. Tew, I. W. Forster, and W. A. Wallace, "Effect of total knee arthroplasty on maximal flexion," *Clinical Orthopaedics and Related Research*, no. 247, pp. 168–174, 1989.

[14] G. Li, E. Most, E. Otterberg et al., "Biomechanics of posterior-substituting total knee arthroplasty: an in vitro study," *Clinical Orthopaedics and Related Research*, no. 404, pp. 214–225, 2002.

[15] Y.-L. Liu, K.-J. Lin, C.-H. Huang et al., "Anatomic-like polyethylene insert could improve knee kinematics after total knee arthroplasty—a computational assessment," *Clinical Biomechanics*, vol. 26, no. 6, pp. 612–619, 2011.

[16] J. V. Baré, H. S. Gill, D. J. Beard, and D. W. Murray, "A convex lateral tibial plateau for knee replacement," *Knee*, vol. 13, no. 2, pp. 122–126, 2006.

[17] J. Bellemans, S. Banks, J. Victor, H. Vandenneucker, and A. Moemans, "Fluoroscopic analysis of the kinematics of deep flexion in total knee arthroplasty," *The Journal of Bone & Joint Surgery B*, vol. 84, no. 1, pp. 50–53, 2002.

[18] Y.-L. Liu, W.-C. Chen, W.-L. Yeh et al., "Mimicking anatomical condylar configuration into knee prosthesis could improve knee kinematics after TKA—a computational simulation," *Clinical Biomechanics*, vol. 27, no. 2, pp. 176–181, 2012.

[19] G. A. Engh, "Failure of the polyethylene bearing surface of a total knee replacement within four years. A case report," *The Journal of Bone & Joint Surgery A*, vol. 70, no. 7, pp. 1093–1096, 1988.

[20] G. A. Engh, K. A. Dwyer, and C. K. Hanes, "Polyethylene wear of metal-backed tibial components in total and unicompartmental knee prostheses," *The Journal of Bone & Joint Surgery B*, vol. 74, no. 1, pp. 9–17, 1992.

[21] J. P. Collier, M. B. Mayor, J. L. McNamara, V. A. Surprenant, and R. E. Jensen, "Analysis of the failure of 122 polyethylene inserts from uncemented tibial knee components," *Clinical Orthopaedics and Related Research*, no. 273, pp. 232–242, 1991.

[22] K. J. Lin, C. H. Huang, W. C. Chen et al., "Joint line elevation would lead to excessive increase of knee stiffness in revision TKA," in *Proceedings of the 56th Annual Meeting of Orthopaedic Research Society*, New Orleans, La, USA, 2010.

[23] J. J. Callaghan, J. N. Insall, A. S. Greenwald et al., "Mobile-bearing knee replacement: concepts and results," *Instructional Course Lectures*, vol. 50, pp. 431–449, 2001.

[24] C.-H. Huang, H.-M. Ma, J.-J. Liau, F.-Y. Ho, and C.-K. Cheng, "Late dislocation of rotating platform in New Jersey low-contact stress knee prosthesis," *Clinical Orthopaedics and Related Research*, no. 405, pp. 189–194, 2002.

[25] C.-H. Huang, H.-M. Ma, J.-J. Liau, F.-Y. Ho, and C.-K. Cheng, "Osteolysis in failed total knee arthroplasty: a comparison of mobile-bearing and fixed-bearing knees," *The Journal of Bone & Joint Surgery A*, vol. 84, no. 12, pp. 2224–2229, 2002.

[26] C.-H. Huang, F.-Y. Ho, H.-M. Ma et al., "Particle size and morphology of UHMWPE wear debris in failed total knee arthroplasties—a comparison between mobile bearing and fixed bearing knees," *Journal of Orthopaedic Research*, vol. 20, no. 5, pp. 1038–1041, 2002.

[27] C.-H. Huang, J.-J. Liau, C.-Y. Lung, C.-T. Lan, and C.-K. Cheng, "The incidence of revision of the metal component of total knee arthroplasties in different tibial-insert designs," *Knee*, vol. 9, no. 4, pp. 331–334, 2002.

[28] K.-J. Lin, C.-H. Huang, Y.-L. Liu et al., "Influence of post-cam design of posterior stabilized knee prosthesis on tibiofemoral motion during high knee flexion," *Clinical Biomechanics*, vol. 26, no. 8, pp. 847–852, 2011.

[29] C.-H. Huang, J.-J. Liau, C.-H. Huang, and C.-K. Cheng, "Influence of post-cam design on stresses on posterior-stabilized tibial posts," *Clinical Orthopaedics and Related Research*, no. 450, pp. 150–156, 2006.

[30] C.-H. Huang, J.-J. Liau, C.-H. Huang, and C.-K. Cheng, "Stress analysis of the anterior tibial post in posterior stabilized knee

prostheses," *Journal of Orthopaedic Research*, vol. 25, no. 4, pp. 442–449, 2007.

[31] Z. W. Wang, Y. L. Liu, K. J. Lin et al., "The effects of implantation of tibio-femoral components in hyperextension on kinematics of TKA," *Knee Surgery, Sports Traumatology, Arthroscopy*, vol. 20, no. 10, pp. 2032–2038, 2012.

[32] K. J. Lin, Y. L. Liu, C. H. Huang et al., "Influence of femoral cam shape on axial tibiofemoral rotation in posterior-stabilized TKA," in *Proceedings of the 57th Annual Meeting of Orthopaedic Research Society*, Long Beach, Calif, USA, 2011.